Cenomanian planktonic foraminifera, bioevents and biozonation – A brief review

Michael D. Bidgood[1]* and Michael D. Simmons[2,3]

With 3 figures and 1 table

Abstract. Cenomanian planktonic foraminifera are important tools for biostratigraphic correlation and calibration to the standard geological timescale. However, their utility is hampered by ambiguity in age calibration, in turn relating to issues of taxonomic identity, potential misidentification, and uncertainty in calibration through association with other fossil groups and proxies such as carbon isotopes. A review of taxonomic and calibration issues suggests that a simple scheme for low to mid latitudes reminiscent of long-established standards is robust. This recognises biozones from oldest to youngest: *Thalmanninella globotruncanoides* Interval Zone (interval from the First Appearance Datum of *Thalmanninella globo-truncanoides* to the First Appearance Datum of *Thalmanninella greenhornensis*; lower Cenomanian); *Thalmanninella greenhornensis* Interval Zone (interval from First Appearance Datum of *Thalmanninella greenhornensis* to First Appearance Datum of *Rotalipora cushmani*; approximately middle Cenomanian); *Rotalipora cushmani* Total Range Zone (interval comprising the total range of *R. cushmani*; upper Cenomanian); *Whiteinella archaeocretacea* Interval Zone (interval from Last Appearance Datum of *R. cushmani* to First Appearance Datum of *Helvetoglobotruncana helvetica*; uppermost Cenomanian – lowermost Turonian). Such a scheme allows for unambiguous correlation and age calibration.

Key words. Cenomanian, planktonic foraminifera, biostratigraphy, biozonation, chronostratigraphy

1. Introduction: The challenges of biostratigraphic calibration and correlation

After over 200 years of practical application, biostratigraphy remains the primary means to achieve geological correlation in sedimentary rocks (McGowran 2005). In turn, this means that biostratigraphy is fundamental to solving geological problems that requires insight into timing and duration. For example, the creation of palaeogeographic maps, development of an understanding of sedimentary architecture, or demonstration of the synchroneity of a geological event such as a sea-level change.

Unfortunately, biostratigraphy is not a simple science (Simmons 2015, Simmons and Bidgood 2022). Founded on taxonomic studies that allow us to distinguish and identify fossil taxa, it requires constantly refining an understanding of inceptions and extinctions, both in a relative sense, and in terms of calibration against the chronostratigraphic standard of geological periods, epochs, and stages. Thus an understanding is created that fossil species A is always found in rocks that are older than those containing fossil species B. A biozonation scheme may be created that uses the inceptions and/or extinctions of fossil species A and B as events defining the boundaries of zones. Such events and zones are, in themselves, useful for correlation, but to aid wider communication, it is

Authors' addresses:
[1] GSS (Geoscience) Ltd, 2 Meadows Drive, Oldmeldrum, AB51 0GA, UK; mike@gssgeoscience.co.uk
[2] Halliburton, 97 Milton Park, Abingdon, OX14 4RW, UK; mike.simmons@halliburton.com
[3] The Natural History Museum, Cromwell Road, London, SW7 5BD, UK
* Corresponding author: mike@gssgeoscience.co.uk

Chronostratigraphy, Tethyan Ammonite & Nannofossil Zones

These zonation schemes redrawn as reproduced in Caron, 1985 - but see text →

Chronostratigraphy, Tethyan Ammonite & Nannofossil Zones				BOLLI 1966 (fide Lehmann, 1966)	PESSA-GNO 1967	POSTUMA 1971	VAN HINTE 1976	SIGAL 1977	ROBASZ-YNSKI & CARON 1979	WONDERS 1980	CARON 1985	SMIRNOV ET AL. 1986	HART ET AL. 1989	SLITER 1989	NEDER-BRAGT 1991
Turonian	M	Collignoniceras woollgari	UC7 (part)	schneegansi I.Z. (part)	renzi (part)	helvetica	sigali + renzi (part)	sigali + schneegansi (part)	helvetica	sigali (part)	helvetica T.R.Z.	imbricata	sigali I.Z. (part)	helvetica	H. globulosa (= reussi)
	E	Mammites nodosoides		helvetica T.R.Z.	helvetica zone (archaeocretacea subz)		helvetica	helvetica		helvetica			helvetica I.Z.		
		Fagesia catinus			helvetica zone (sigali subzone)				archaeo-cretacea		archaeo-cretacea I.Z.			archaeo-cretacea	
		Watinoceras devonense	UC6	gigantea I.Z.	[no name assigned]		lehmanni			archaeo-cretacea	archaeo-cretacea I.Z.		archaeo-cretacea I.Z.		
Cenomanian	Lt	Neocardioceras juddii	UC5c / UC5b / UC5a	cushmani T.R.Z.	Rotalipora s.s. zone (cushmani + greenhornnensis subz)	cushmani	cushmani	cushmani	cushmani	cushmani	cushmani T.R.Z.	deeckei - portsdownensis	cushmani T.R.Z.	cushmani	
		Metoicoceras geslinianum	UC4b / UC4a / UC3e												
		Calycoceras guerangeri	UC3d / UC3c												
	M	Acanthoceras jukesbrownei	UC3b	reicheli I.Z.		greenho-rnensis	reicheli + gandolfii		reicheli	reicheli T.R.Z.		reicheli T.R.Z.	reicheli	
		Acanthoceras rhotomagense	UC3a												
		C. inerme													
		Mantelliceras dixoni	UC2c			appenninica		globotruncanoides + brotzeni				brotzeni - planispira			
	E		UC2b	brotzeni I.Z.	Rotalipora s.s. zone (evoluta subzone)		gandolfii + greenhornensis		brotzeni	globotruncanoides	brotzeni I.Z.		appenninica I.Z.	brotzeni	H. moremani
			UC2a												
		Mantelliceras mantelli	UC1c			buxtorfi						appenninica - caspia			
			UC1b							appenn. s.l.					
			UC1a												
		Arrhaphoceras briacensis	UC0b	appenninica I.Z.	[no zones assigned]	breggiensis	appenninica + buxtorfi	appenninica + buxtorfi	appenninica	appenninica + buxtorfi	appenninica I.Z.	infracretacea	[no zones assigned]	appenninica	
Albian	Lt	Praeschloen-bachia perinflatum	UC0a (part)				ticinensis + buxtorfi			ticinensis + buxtorfi					
		Praeschl. rostratum													
		Pervenquieria fallax		ticinensis I.Z. (part)		breggiensis (part)	breggiensis (part)	breggiensis (part)	ticinensis (part)	praebuxtorfi (part)	ticinensis I.Z. (part)				

The "GTS Family" of zonation schemes

Chronostratigraphy, Tethyan Ammonite & Nannofossil Zones				ROBASZYNSKI & CARON 1995	SALAJ 1996	HARDENBOL ET AL. 1998	TUR ET AL. 2001	PREMOLI SILVA & VERGA 2004	GTS 2004/8	GTS 2012	GTS 2016	GTS2020 fide COCCIONI & PREMOLI SILVA 2015	GEORGESCU 2017	PETRIZZO & GILARDONI 2020 & PETRIZZO et al. 2021
	Turonian	M	*Collignoniceras woollgari* UC7 (part)	*schneegansi* I.Z. (part)	*schneegansi* (part)	*schneegansi* I.Z. (part)	*coronata* I.Z. (part)	*sigali - primitiva* I.Z. (part)	*schneegansi* I.Z. (part)	*schneegansi* I.Z. (part)	*schneegansi* I.Z. (part)	*schneegansi* I.Z. (part)	*helvetica* T.R.Z.	*schneegansi* I.Z. (part)
				helvetica T.R.Z	*helvetica*	*helvetica* T.R.Z	*helvetica* T.R.Z	*helvetica* T.R.Z	*helvetica* T.R.Z	*helvetica* T.R.Z	*helvetica* T.R.Z	*helvetica* T.R.Z		*helvetica* T.R.Z
		E	*Mammites nodosoides*												
			Fagesia catinus		*archaeo-cretacea*	*helvetica* T.R.Z			*archaeo-cretacea* I.Z.	*archaeo-cretacea* I.Z.	*archaeo-cretacea* I.Z.	*archaeo-cretacea* I.Z.	*G. carpathica* I.Z.	*archaeo-cretacea* I.Z.
			Watinoceras devonense UC6	*archaeo-cretacea* I.Z.			*archaeo-cretacea* I.Z.	*archaeo-cretacea* I.Z.					*P. turbinata* I.Z.	
	Cenomanian	Lt	*Neocardioceras juddii* UC5c / UC5b / UC5a			*archaeo-cretacea* I.Z.								
			Metoicoceras geslinianum UC4b / UC4a		*cushmani*	*cushmani* T.R.Z.	*cushmani* T.R.Z.	*cushmani* T.R.Z.	*cushmani* T.R.Z.	*cushmani* T.R.Z.	*cushmani* T.R.Z.	*cushmani* I.Z.	*H. mihaii* I.Z.	*cushmani* T.R.Z.
			UC3e / UC3d	*cushmani* T.R.Z.										
			Calycoceras guerangeri UC3c / UC3b											
		M	*Acanthoceras jukesbrownei*										*cushmani* I.Z.	
			Acanthoceras rhotomagense UC3a	*reicheli* I.Z.	*bicarinata evoluta*	*reicheli* I.Z.	*reicheli* I.Z.	*reicheli* T.R.Z.	*reicheli* I.Z.	*reicheli* I.Z.	*reicheli* I.Z.	*cushmani* I.Z.		*greenhornensis* I.Z.
			C. inerme		*deeckei*									
			Mantelliceras dixoni UC2c / UC2b	*globotruncanoides* I.Z.	*gandolfii*	*globotruncanoides* I.Z.	*globotruncanoides* I.Z.	*globotruncanoides* I.Z.	*globotruncanoides* I.Z.	*globotruncanoides* I.Z.	*globotruncanoides* I.Z.	*globotruncanoides* I.Z.	*micheli* I.Z.	*globotruncanoides* I.Z.
		E	UC2a											
			Mantelliceras mantelli UC1c		*brotzeni*							*reicheli* T.R.Z.		
			UC1b / UC1a											
	Albian	Lt	*Arrhaphoceras briacensis* UC0b	*appenninica* I.Z.	[no zones assigned]	*appenninica* I.Z.	*appenninica* I.Z.	*appenninica* I.Z.	*appenninica* I.Z.	*appenninica* I.Z.	*appenninica* I.Z.	*appenninica* I.Z.	*appenninica* I.Z.	*appenninica* I.Z.
			Praeschloenbachia perinflatum UC0a (part)											
			Praeschl. rostratum											
			Pervenquieria fallax	*ticinensis* I.Z. (part)	*ticinensis* I.Z. (part)	[no zones assigned]	*ticinensis* I.Z. (part)	*ticinensis* I.Z. (part)	*ticinensis* I.Z. (part)	*ticinensis* I.Z. (part)	*ticinensis* I.Z. (part)	*ticinensis* I.Z. (part)	Not Zoned	*ticinensis* I.Z. (part)

Fig. 1. a, b: Historical development of Cenomanian planktonic foraminiferal biozonation. Horizontal lines are drawn according to ammonite calibration in the original schemes (dashed if uncalibrated). (IZ = Interval Zone, TRZ = Total Range Zone. Timescale, chronostratigraphy, ammonite and nannofossil zones derived from Time Scale Creator ver. 8.0).

usually desirable to calibrate to the standard chronostratigraphy that all geoscientists are aware of. Ultimately, this enables a biostratigrapher to assert that a given rock succession is, for example, Cenomanian in age, or lower Cenomanian, etc.

Despite the publication of charts that suggest that the process of bioevent and biozone calibration is well understood (see examples in the Geological Time Scale of Gradstein et al. 2020 (GTS2020) and associated software 'Time Scale Creator' – https://timescalecreator.org/), this may not always be the case. Bulot et al. (2022), following data published by Luber et al. (2019), noted that for Aptian strata in Morocco, the calibration of planktonic foraminifera and calcareous nannofossil events to the ammonite biozonation was not what might have been expected. Ambiguity and lack of consensus can often exist. As an example, one of the charts illustrating the Cretaceous chapter of GTS2020 (Gale et al. 2020) shows the base of the well-known *Rotalipora cushmani* planktonic foraminifera zone as occurring low within the Cenomanian (following Premoli Silva and Sliter 1995 and Coccioni and Premoli Silva 2015). There is another and perhaps more widely accepted view (e. g., Petrizzo and Gilardoni 2020), that this boundary occurs much higher in the Cenomanian. It can be appreciated that differing versions of biozone boundary placement calibration will have profound impacts on the correlation of rocks and geological events that relate to this bioevent.

There are many reasons why biostratigraphic calibration is not straightforward. These include taxonomic uncertainties regarding identity (Corbett et al. 2014, Falzoni et al. 2018), and misidentifications falsely extending stratigraphic range (Schlagintweit and Simmons 2022); and most importantly, lack of direct calibration between biostratigraphic schema. For example, some marine sediments containing planktonic foraminifera and calcareous nannofossils have a particularly poor ammonite fauna, such as the chalk facies of Europe (Gale et al. 2020). Endemism can create further calibration issues. Moreover, it has long been recognised that in reality the inception and extinction of species are diachronous events (Simpson 1951, Pearson 1998, Simmons and Bidgood 2022). In many cases, the diachroneity is insufficient to be significant (i. e., to prevent reliable correlation), in other cases it is significant (Falzoni et al. 2018).

Precise biostratigraphic calibration and correlation are important for any period during the Phanerozoic history of the Earth, but herein we focus on the Cenomanian stage of the mid-Cretaceous. The Cenomanian represents an intriguing episode in the sedimentary, geodynamic, and biological history of the planet, and it contains rocks of major economic importance. Events within and around the Cenomanian such as short-term sea-level change (Haq 2014, Ray et al. 2019), expansion and demise of carbonate platforms and associated fauna (Philip and Airaud-Crumiere 1991, Höfling and Scott 2002, Johnson 2002, Johnson et al. 2002, Steuber et al. 2016, Rineau et al. 2021), and ocean anoxia (Jenkyns 2010, Joo and Sageman 2014, Gambacorta et al. 2015, Laugié et al. 2021) require a robust framework for correlation. One of the tools that has traditionally been used for correlation is planktonic foraminifera biostratigraphy (Fig. 1), given the widespread occurrence of rapidly evolving and stratigraphically restricted species during the mid-Cretaceous. Yet as already stated, there is ambiguity and lack of consensus (e. g., Coccioni and Premoli Silva 2015 vs Petrizzo and Gilardoni 2020) on the calibration of biozone and bioevents (Simmons 2021). Indeed, it could be argued that despite decades of research, Cenomanian planktonic foraminifera typify all the challenges that need to be overcome to establish robust calibration – agreement on taxonomy, stratigraphic ranges, and calibration to the zonations of other fossil groups and the chronostratigraphic standard. Herein we review these issues that can be confusing to follow in the literature and make recommendations for a likely consensus.

2.   The Cenomanian stage

The biostratigraphy of the Cenomanian stage has been intensively studied since its introduction in 1847 by Alcide d'Orbigny (Morel 2015). Formal definition of the boundary of the Cenomanian with the overlying Turonian stage (key proxy event: lowest occurrence of the ammonite *Watinoceras devonense* Wright and Kennedy) occurred in 2003 (Kennedy et al. 2005), with a Global Stratigraphic Section and Point (GSSP) section at Pueblo, Colorado, USA. Formal definition of the boundary of the Cenomanian with the underlying Albian stage (key proxy event: lowest occurrence of the planktonic foraminifera *Thalmanninella globotruncanoides* (Sigal)) occurred in 2002 (Kennedy et al. 2004), with a GSSP section at Mont Risou, France, although this defining bioevent had been proposed and agreed much earlier (Gale et al. 1996, Tröger and Kennedy 1996).

The formal GSSP-based definitions of the Cenomanian stage boundaries, mean some rock units previously regarded as uppermost Cenomanian will now be regarded as lowermost Turonian, and that some rock units previously regarded as uppermost Albian, will now be regarded as lowermost Cenomanian. For example, in Europe, the base of the Cenomanian had traditionally been drawn at the first appearance datum (FAD) of the genus *Mantelliceras* Hyatt (typically the species *Mantelliceras mantelli* (J. Sowerby)) (e.g., Gale 1995, Hardenbol et al. 1998). This is now positioned *within* the lower Cenomanian (Gale et al. 2020). The changing nature of the stage boundaries needs to be considered when referring to older literature, especially regarding the age of lithostratigraphic units or the stratigraphic range of fossils.

The Cenomanian is typically subdivided into three substages: lower, middle, and upper, although as yet there is no formally accepted definition for the base of the middle Cenomanian or upper Cenomanian. Nonetheless, the base of the middle Cenomanian is traditionally taken at the base of the *Cunningtoniceras inerme* ammonite biozone (e.g., Tröger and Kennedy 1996, Hardenbol et al. 1998, Kennedy and Gale 2017, Wright et al. 2017). This is equivalent to the base of the *Conlinoceras tarrantense* Zone of the Western Interior Basin (WIB) in North America. The base of the upper Cenomanian can be taken as the base of the *Calycoceras guerangeri* Zone (Hardenbol et al. 1998, Wright et al. 2017) associated with the replacement of ammonites of the genus *Acanthoceras* by the genus *Calycoceras* Hyatt (Hancock 1991). The *C. guerangeri* Zone is approximately coeval with the base of the *Dunveganoceras pondi* Zone in the WIB (Cobban et al. 2006).

A widely accepted estimate for the duration of the Cenomanian is 6.6 Myr (Gale et al. 2020) based on radiometric isotope ages, although Beil et al. (2018) calculated a 4.8 Myr duration based on recognition of orbital forcing cycles. The Beil et al. work (using a core from Morocco) is based on the premise that the core represents a complete, uninterrupted, Cenomanian deposit through which counts of sedimentary cycles (representing the 405 kyr cycle) can be made. However, this is not convincingly demonstrated from the associated biostratigraphy. In summary, the base of the Cenomanian is associated with an age of 100.5 Ma based on extrapolation of dated tuffs from Hokkaido, Japan (Obradovich et al. 2002, Takashima et al. 2019, Schmitz 2020), whilst the age of the Cenomanian – Turonian boundary is well-constrained as 93.9 ±0.2 Ma by $^{40}Ar/^{39}Ar$ ages from bentonites close to the GSSP section in Colorado (Obradovich 1993, Meyers et al. 2012).

The informal substages of the Cenomanian are not evenly spaced, with the lower Cenomanian representing almost two-thirds of the duration of the stage (Gale et al. 2020). Substage and zonation durations are in part estimated using cyclostratigraphy, including recognition of the 405-kyr orbital forcing cycle. For example, the duration between the carbon isotope events near the base of the middle Cenomanian ('MCE II') and that within the upper Cenomanian ('OAE2 peak B' – see Fig. 2), is estimated at approximately 1.9 Myr. This is supported by radiometric dating of bentonites from near the base of the middle Cenomanian in the WIB as 96.21 ± 0.36 Ma (Gale et al. 1999, Eldrett et al. 2015, Batenburg et al. 2016) and other intra-Cenomanian radiometric dates (e.g., Cobban et al. 2006, Schmitz 2020). The base of the upper Cenomanian appears to be slightly older than 95.39 Ma (+/- 0.37) – a radiometric age from a sample assigned to the *D. pondi* ammonite zone of the WIB (Schmitz 2020). The boundary is placed at 95.47 Ma by Gale et al. (2020).

The Cenomanian represents a remarkable time during Earth's history. Climates are typically regarded as relatively warm (Francis and Frakes 1993, Skelton 2003, Hart 2007, Hong and Lee 2012, O'Brien et al. 2017, Laugié et al. 2020, Scotese et al. 2021) and sea-levels as relatively high (Haq et al. 1987, McDonough and Cross 1991, Haq 2014, Vérard et al. 2015, van der Meer et al. 2017, Simmons et al. 2020, Wright et al. 2020). On the other hand, there is growing evidence for significant short-term eustasy (e.g., Haq et al. 1987, Sahagian et al. 1996, Robaszynski et al. 1998, Scott et al. 2018, Hancock 2004, Miller et al. 2004, Simmons et al. 2007, Kominz et al. 2008, van Buchem et al. 2011, Haq 2014, Ray et al. 2019), possibly linked to ephemeral ice sheets waxing and waning (Miller et al. 2003, Miller et al. 2005, Voigt et al. 2006, Plint and Kreitner 2007, Koch and Brenner 2009, Ladant and Donnadieu 2016, Davies et al. 2020), and/or other eustatic drivers (Wendler and Wendler 2016, Sames et al. 2016, Sames et al. 2020), since the $\delta^{18}O$ record appears stable across certain events (Ando et al. 2009). Orbital forcing of global climate is clearly present in the Cenomanian (Gale et al. 1999, Gale et al. 2002, Gale et al. 2008, Wendler et al. 2010, Wendler et al. 2014, Boulila et al. 2011, Al-Husseini 2018, Huang 2018) and is very likely linked to short-term eustasy.

Significant geodynamic developments were taking place during the Cenomanian (Stampfli and Borel

2002, Giorgioni et al. 2015, Torsvik and Cocks 2017, Laugié et al. 2021, Scotese 2021), with the onset of the closure of Tethys and the opening of the Atlantic. Excursions in the carbon cycle are a notable feature of the mid-Cretaceous (Coccioni and Galeotti 2003, Jarvis et al. 2006, Cramer and Jarvis 2020) and include ocean anoxic events (OAEs) 1d and 2 (Jenkyns 2010, Joo and Sageman 2014, Gambacorta et al. 2015, Laugié et al. 2021) that lie close to the boundaries of the Cenomanian stage. Cenomanian sediments also have significant economic potential. For example, petroleum source rocks are developed during times of anoxia, and reservoir rocks were created within the widespread carbonate platforms that typify the stage (Scott et al. 1993, Alsharhan and Scott 2000, Marlow et al. 2014, Esrafili-Dizaji and Rahimpour-Bonab 2019, Bromhead et al. 2022).

The Cenomanian represents a period of significant faunal and floral diversity. The relatively warm climate and relatively high long-term eustatic sea-level led to widespread carbonate platform development where many organisms proliferated and diversified (Philip and Airaud-Crumiere 1991, Höfling and Scott 2001, Johnson 2002, Johnson et al. 2002, Steuber et al. 2016, Rineau et al. 2021). These included larger benthic foraminifera and rudist bivalves. In the relatively deep waters of the open shelves and basins, ammonites, inoceramid bivalves, planktonic foraminifera, calcareous nannofossils, and dinoflagellates proliferated and diversified. In all settings, several fossil groups displayed rapid evolutionary trends, with several species or genera having short stratigraphic ranges making them useful for biostratigraphy. These evolutionary patterns were linked to short-term climatic, eustatic and oceanographic events (Mitchell and Carr 1998), not least the OAEs and their precursors that lie within and close to the boundaries of the Cenomanian stage (Jarvis et al. 1988).

3.   Cenomanian planktonic foraminifera

Following a major evolutionary radiation at the beginning of the Albian, mid-Cretaceous planktonic foraminifera were diverse, with a number of important inception and extinction events that are the basis for biozonation (see subsequent detailed discussion), and which are useful for practical interregional correlation in suitable facies. During the Cenomanian trochospiral

taxa diversified, and forms with coarse pustules (*Whiteinella* Pessagno), and with a single keel (*Rotalipora* Brotzen) appeared, along with the double-keeled *Dicarinella* Porthault, and *Marginotruncana* Hofker in the upper Cenomanian. A significant change occurs across the Cenomanian – Turonian boundary with the last *Rotalipora* (*Rotalipora cushmani* (Morrow)) becoming extinct shortly after the onset of OAE 2 within the upper Cenomanian (e. g., Falzoni et al. 2018). As with many other fossil groups, climate change and oceanic anoxic events exerted a strong control on evolutionary episodes in planktonic foraminifera in the mid-Cretaceous.

Rotaliporids (i. e., Rotaliporidae), have variously comprised the genera *Anaticinella* Eicher, *Biticinella* Sigal, *Pseudorotalipora* Ion, *Pseudothalmanninella* Wonders, *Pseudoticinella* Longoria *Parathalmanninella* Lipson-Benitah, *Rotalipora* Brotzen, *Thalmanninella* Sigal, and *Ticinella* Reichel – see, for example, Lipson-Benitah (2008) and Huber et al. (2016), but see also Gonzalez-Donoso et al. (2007) who retained only three genera within the family – *Pseudothalmanninella*, *Thalmanninella* and *Rotalipora*). They are the most important biostratigraphic markers in the Cenomanian in tropical-warm temperate regions (many of the taxa discussed below are not found in higher latitudes where other zonation schemes may be applied). However, few fossil groups have undergone a more convoluted history of taxonomic description, re-description, and re-definition between and within species. The family Rotaliporidae (Sigal) includes two subfamilies – the Rotaliporinae (Sigal) and the Ticinellinae (Longoria) – as per the classification of Loeblich and Tappan (1988). The Rotaliporinae subfamily are keeled, even if only developed on earlier chambers of the final whorl, e. g., as in *Thalmanninella praebalernaensis* (Sigal), or incomplete (i. e., weakly developed and possibly absent on later chambers) as in the terminal genus *Anaticinella*), and the Ticinellinae are unkeeled. In general, it is mostly members of the Rotaliporinae subfamily that are biostratigraphically useful in the Cenomanian.

The most recent position (e. g., 'Microtax' (Huber et al. 2016)) is a Rotaliporidae family comprising six genera: *Anaticinella*, *Biticinella*, *Pseudothalmanninella*, *Rotalipora*, *Thalmanninella* and *Ticinella* and a total of 28 species.

There are, depending on authors, either two or three evolutionary lineages within these rotaliporids (see Ando and Huber 2007, Gonzalez-Donoso et al. 2007). Morphological variation within species is high

(Ando and Huber 2007) and intermediate/transitional morphologies between species are also very common. This accounts for many of the taxonomic/evolutionary/biostratigraphic controversies over the past decades. A full discussion on evolutionary relationships between taxa is not included here except for a few specific instances in the text below.

Navigating the taxonomic literature on Cenomanian planktonic foraminifera is difficult because no authors have treated the rotaliporids collectively, and disagreements between authors are frequent. Some publications adopt a contrary position to others at one time, only to seemingly agree in later publications (or vice versa), but this probably reflects the undoubted (but slow) progress being made on this topic. Comprehensive atlases with modern and fully revised planktonic foraminiferal taxonomies, such as ones produced for the Paleocene (Olsson et al. 1999), Eocene (Pearson et al. 2006) and Oligocene (Wade et al. 2018) have not been forthcoming for Cretaceous taxa since the 1970s and 1980s. The following publications (in alphabetical order) are not exhaustive but are suggested reading. They include works concerning primarily Cenomanian planktonic foraminifera and works that include Cenomanian within analysis of longer stratigraphic intervals: Ando and Huber 2007, Ando et al. 2009, Ando et al. 2015, Bolli 1966, Caron 1985, Bralower et al. 1995, Caron and Premoli Silva 2007, Caron and Spezzaferri 2006, Caron et al. 2006, Coccioni and Galeotti 2003, Coccioni and Premoli Silva 2015, Coccioni et al. 2006, Desmares et al. 2007, Desmares et al. 2016, Desmares et al. 2019, Erbacher et al. 2020, Falzoni et al. 2016, Falzoni et al. 2018, Gale et al. 1996, Gale et al. 2002, Gale et al. 2011, Gale et al. 2019, Gale et al. 2020, Gale et al. 2021, Georgescu 2017, Gilardoni 2017, Gonzalez-Donoso et al. 2007, Hardenbol et al 1998, Hart 2021, Hart et al. 1989, Haynes et al. 2015, Huber and Petrizzo 2014, Huber et al. 2016, Huber et al. 2017, Huber et al. 2022, Keller and Pardo 2004, Keller et al. 2008, Kennedy et al. 2004, Kennedy et al. 2005, Leary et al. 1989, Leckie et al. 2002, Lipson-Benitah 2008, Lowery and Leckie 2017, Luciani and Cobianchi 1999, Morel and Desmares 2017, Nederbragt 1991, Ogg and Hinov 2012, Ogg et al. 2004, Ogg et al. 2008, Ogg et al. 2016, Paul et al. 1994, Pessagno 1967, Petrizzo and Gilardoni 2020, Petrizzo and Huber 2006, Petrizzo et al. 2015, Petrizzo et al. 2021, Postuma 1971, Premoli Silva and Sliter 1995, Premoli Silva and Verga 2004, Robaszynski and Caron 1979, Robaszynski and Caron 1995, Robaszynski et al. 1990, Robaszynski et al. 1993a, Robaszynski et al. 1993b, Robaszynski et al. 1998, Robaszynski et al. 2005, Robaszynski et al. 2008, Robaszynski et al. 2010, Salaj 1996, Scopelliti et al. 2004, Scopelliti et al. 2008, Sigal 1977, Sliter 1989, Spezzaferri and Caron 2008, Smirnov et al. 1986, Sprovieri et al. 2013, Troger and Kennedy 1996, Tur et al 2001, Van Hinte 1976, Wagreich et al. 2008, Wonders 1978, Wonders 1980.

The first published planktonic foraminiferal biozonation scheme to include the Cenomanian was that of Bolli (1966). However, during subsequent decades, periodic major revisions on the taxonomy of Cenomanian rotaliporids have resulted in the proliferation of more-or-less different biostratigraphic schemes or re-definitions of existing zones (Fig. 1).

Many of the early schemes did not attempt calibration to independent chronostratigraphic/age-significant markers such as ammonite (or other fossil type) zones or stable isotope data. Zonation boundaries were often drawn co-incident with stage boundaries or arbitrarily assigned visually approximate separations from one another. One of the first schemes to attempt calibration was that of Robaszynski and Caron (1979) who proposed biozones calibrated to European ammonite zones which effectively became the basis of most subsequent zonations, albeit with some modifications and progressive calibration adjustments. They further revised their scheme in 1995 and the essential elements of this can still be seen in important global timescale references such as Hardenbol et al. 1998 (sometimes referred to as 'SEPM 1998') and the 'family' of Geological Time Scale publications GTS2004 (Ogg et al. 2004), GTS2008 (Ogg et al. 2008), GTS2012 (Ogg and Hinnov 2012) and GTS2016 (Ogg et al. 2016) but not GTS2020 (Gale et al. 2020). Slight calibration changes seen in successive GTS schemes are due to adjustments (often based on cyclo-stratigraphy) suggested by workers communicating informally to the GTS editorial team. Many/most of these suggestions can be viewed as 'popups' in the various Time Scale Creator datapack versions.

Nannofossil zones (the 'UC' scheme of Burnett 1998) are included in Figures 1 and 2 for reference but it should be noted that nannofossil taxonomy and biostratigraphy in the Cenomanian is also in need of review as no new/revised Cenomanian zonation scheme has been published in the 21st century. Figure 1 shows that the biostratigraphic resolution afforded by nannofossils (5 zones) is only slightly greater than that afforded by planktonic foraminifera (4) at the zonal level. However, there are more defined nannofossil

Table 1. Foraminiferal biozonation definitions and ages for the Cenomanian and adjacent intervals as used herein (see also Fig. 2).

Zone	Defined by	Age
Helvetoglobotruncana helvetica Total Range Zone	Interval comprising the total range of *H. helvetica*	lower – middle Turonian
Whiteinella archaeocretacea Interval Zone	Interval from LAD (Last Appearance Datum) of *R. cushmani* to the FAD of *H. helvetica*	uppermost Cenomanian – lowermost Turonian
Rotalipora cushmani Total Range Zone	Interval comprising the total range of *R. cushmani*	upper middle to upper Cenomanian
Thalmanninella greenhornensis Interval Zone	Interval from FAD of *T. greenhornensis* to the FAD of *R. cushmani*	approximately upper lower – lower middle Cenomanian
Thalmanninella globotruncanoides Interval Zone	Interval from the FAD of *T. globotruncanoides* to the FAD of *T. greenhornensis*	lower Cenomanian
Thalmanninella appenninica Interval Zone	Interval from the FAD of *T. appenninica* to the FAD of *T. globotruncanoides*	uppermost Albian

subzones throughout the Cenomanian, whereas planktonic foraminiferal subzones (where defined) occur only in the upper Cenomanian-lower Turonian interval (see below). These nannofossil zonal and subzonal markers are not always observed however. For example, Tremolada (2002) was only able to distinguish two intervals; UC0 and UC1-UC5, in the Cenomanian Scaglia Bianca at Gubbio, Italy (see below). The nannofossil event closest to the base of the Cenomanian is the FAD of *Corolithion kennedyi* Crux, marking the base of zone UC1, which occurs slightly above the GSSP marker for the stage – the FAD of *T. globotruncanoides*. The event is somewhat younger in Boreal realms (Burnett 1998).

Higher resolution nannofossil studies have been carried out in the upper part of the Cenomanian of the WIB (e. g., Corbett et al. 2014) which shows some disagreement with events published by Burnett (1998). The Cenomanian-Turonian boundary is marked by the FAD of the nannofossil *Quadrum gartneri* Prins & Perch-Nielsen, although there is some disagreement among workers as to its exact placement with respect to ammonite zones which range from within *juddi* (Hardenbol et al. 1998), within *devonense* (Huber and Petrizzo 2014 – as shown herein), top *devonense* (Watkins in TSC ver. 8.0) and within *nodosoides* (Burnett 1998).

In this work we suggest the following planktonic foraminiferal biozonation (Table 1) for the interval under study should be adopted, based on Petrizzo and Gilardoni 2020 (for the 'lower' part of the Cen-

omanian) and Robaszynski and Caron 1995 (for the 'upper' part of the Cenomanian).

Discussions below will refer to these biozones and biozones of others (in particular the *Thalmanninella reicheli* Zone which is, to a degree, replaced by the *T. greenhornensis* zone).

Defining the *reicheli* and *cushmani* zones as variously Interval or Total Range Zones has also led to potential confusion. The current iteration of the 'standard' zonation (Coccioni and Premoli Silva 2015 as adopted in GTS2020, Gale et al. 2020 see Fig. 1 herein) is at major odds with previous interpretations with, for example, the *cushmani* Zone now occupying much of the entire Cenomanian, and the *reicheli* Zone now low in the lower Cenomanian, rather than being placed in the middle Cenomanian.

Schemes that do not rely on rotaliporids as primary marker species (e. g., Nederbragt 1991 *fide* Robaszynski and Caron 1995, Georgescu 2017) are also proposed although seldom cited. For example, Georgescu (2017) uses the FADs of *Heterohelix mihaii* and *Globotruncanita carpathica* Scheibnerova (now in synonymy with *Helvetoglobotruncana helvetica*) to define his nominal biozones in the upper Cenomanian and lowermost Turonian respectively.

Further refinement of the standard zonation, especially around the Cenomanian-Turonian boundary interval (OAE2) of a section in Morocco has been proposed by Keller et al. (2008) with the *R. cushmani* and *W. archaeocretacea* zones being subdivided into 3 subzones each (see Keller et al. 2008 – fig. 4):

W. archeocretacea Zone	*H. moremani* Subzone (the chronostratigraphic Cenomanian-Turonian boundary occurs within this subzone)
	D. hagni Subzone
	G. bentonensis Subzone
R. cushmani Zone	*Rotalipora* extinction Subzone
	A. multiloculata Subzone
	P. praehelvetica Subzone

However, the apparent variability of environmental conditions at this time around the world suggests few, if any, of the zone-defining events may be synchronous globally or perhaps even regionally (Falzoni et al. 2018). For example, the FADs of *H. helvetica* and some *Dicarinella* species, the LAD of the anaticinellids and the onset of the 'heterohelicid shift' are diachronous in three sections (Pueblo, USA; Eastborne, UK; and Tarfaya, Morocco) as determined by graphic correlation, and by observation in others (Vocontian Basin, France; Wadi Bahloul, Tunisia; Gongzha, Indian Ocean). The positions of the 'heterohelicid shift' and the FAD of *Dicarinella elata* are ecologically controlled and the (apparently diachronous) FAD of *H. helvetica* is mainly due to taxonomic uncertainties and/or differing species concepts (see Falzoni et al. 2018, Fig. 9).

4. Taxonomy, species concepts and identification of biostratigraphically useful taxa

The majority of potentially valid species of rotaliporids, along with several other stratigraphically useful Cenomanian planktonic foraminifera taxa, were discovered and described before the mid-1970s. However, polyphyleticism and taxonomic controversies – particularly synonymy and different species concepts between researchers due to high morphological variability (almost all evolutionary and some unrelated pairs contain transitional forms) – have bedevilled the group ever since. The differences, for example, between such subjective terms as "strongly raised sutures" or "normally raised sutures" or "partly raised sutures" in the definition and separation of certain species has not been established (Ando and Huber 2007). The issue of taxonomic stability is gradually being resolved (e. g., Huber et al. 2022 for planispiral forms) but the discussion often remains rather impenetrable for the non-specialist and even for other foraminiferal workers.

Taxonomic controversies, together with misidentifications, peculiarities of individual sections from which zonations are developed and sample size/frequency (Falzoni et al. 2018) are responsible for much of the fluidity and/or fuzziness of Cenomanian biozones. This situation is gradually being resolved (Ando and Huber 2007, Gonzalez-Donoso et al. 2007, Petrizzo et al. 2015, Falzoni et al. 2018, Petrizzo and Gilardoni 2020, Petrizzo et al. 2021) but problems remain. Even when taxonomic/identification issues have been settled, diachronism of inception and extinction events is also readily apparent (e. g., Desmares et al. 2007, Falzoni et al. 2018). Specific (but certainly not all) issues are discussed below.

Species are here assigned to genera following the position adopted in 'Mikrotax' online (https://www.mikrotax.org/index.php – Huber et al. 2016) at the time of writing, for example the commonly-known species *Globigerinelloides bentonensis* (Morrow) has been very recently re-assigned to the new genus, *Laeviella* (Huber et al. 2022). Illustrations – particularly type material – of taxa mentioned throughout the text can also be found on that website, along with information on stratigraphic ranges. Comments on uncertainty of these ranges are included in the text.

A full taxonomic revision inclusive of all rotaliporids and their allies is necessary, but far beyond the scope of this paper, as is a full history of zonation development and evolutionary relationships between taxa, but a table of the pertinent taxa, together with remarks on their current taxonomic and biostratigraphic status, is provided as Appendix 1. However, several of these entries may still be disputed. Ranges shown in Appendix 1 and events shown on Fig. 2 are considered likely maximums although locally ranges may not achieve their full expression. Non-rotaliporid biostratigraphic events are based on ranges from Premoli Silva and Verga 2004, 'Mikrotax' – Huber et al. 2016 and TSCPro 8.0

4.1. *Thalmanninella globotruncanoides* and *Thalmanninella brotzeni*

The first Cenomanian zonation scheme (Bolli 1966, *fide* Lehmann 1966, see Fig. 1) used the First Appearance Datum (FAD) of *Thalmanninella brotzeni* Uk crl' to define the base of the *brotzeni* Zone calibrated to the lower Cenomanian (and essentially picking the base of the Cenomanian in foraminiferal terms). *T. brotzeni* has been placed in synonymy with other taxa (e. g., *Thalmanninella greenhornensis* (Morrow), Wonders 1980). Ando and Huber (2007) also remark "… *R. brotzeni* is reminiscent of *R. greenhornensis* as judged from its type figure…", and for a period of time *T. globotruncanoides* and *T. brotzeni* were regarded as synonyms, with the former species considered as the senior synonym (e. g., Robaszynski et al. 1993, Robaszynski et al. 2008, Gonzalez-Donoso et al. 2007, Ando and Huber 2007). This position was adopted when the Global Stratigraphic Section and Point (GSSP) of the base Cenomanian was defined (Kennedy et al. 2004) by the FAD of *T. globotruncanoides* at Mont Risou in France.

Meanwhile, Caron and Premoli Silva (2007) re-examined original type material and concluded that the two taxa were not synonymous, a position confirmed and expanded upon by Petrizzo et al. 2015 (who also confirmed the status of *T. greenhornensis* as a separate species as confirmed earlier by Ando and Huber 2007). Using the revised definitions, workers have concluded that the FAD of *T. brotzeni* precedes that of *T. globotruncanoides* (Petrizzo et al. 2015, Petrizzo and Gilardoni 2020, Gale et al. 2021, Arany 2021, pers. comm., although see Huber et al. 2016 – 'Mikrotax' who place the FAD of *T. brotzeni* "within the *T. globotruncanoides* zone"). However, Petrizzo et al. (2015) confirmed the FAD of true (i. e., as currently defined and *not* including *T. brotzeni*) *T. globotruncanoides* at –36 m at Mont Risou, the same sample used to define the base Cenomanian GSSP by Kennedy et al. (2004).

4.2. *Thalmanninella greenhornensis*

Thalmanninella greenhornensis is often confused with its ancestor *T. globotruncanoides* (and was occasionally placed in synonymy with it (e. g., Caron 1985). Ando and Huber (2007) recognise intermediate forms between the two which they say may justify the establishment of a new species, although Gilardoni (2017) found no transitional forms in her studies.

Thalmanninella greenhornensis has also been synonymised with *T. brotzeni* (Wonders 1980). Gonzalez-Donoso et al. (2007) identified an additional form "*T. greenhornensis* umbilico-convex", differing in profile view only but belonging to a different lineage. Ando and Huber (2007) provided a major taxonomic revision of this species and its associates thus providing some clarity. However, Ando and Huber (2007) stated the range of *T. greenhornensis* was essentially equivalent to the upper Cenomanian *R. cushmani* Zone only. The FAD of *T. greenhornensis* defines the upper lower to lower middle Cenomanian (on the basis of an association with the Mid Cenomanian Excursion (MCE) δ^{13}C isotope peaks) *greenhornensis* Zone of Petrizzo and Gilardoni (2020) – a 'replacement' for the long-established *reicheli* Zone – a suggestion originally proposed by Postuma (1971), but which appears to have been largely ignored until recently. The nominate species is much more abundant and widespread than *T. reicheli* (see below) but is not universally recorded (e. g., Tur et al. 2001).

The FAD event of *T. greenhornensis* (and by association, the FAD of *T. reicheli*) is difficult to calibrate precisely to the timescale but occurs approximately 10 m below the MCE event at Monte Petrano (Petrizzo and Gilardoni 2020). As the MCE begins in the *inerme* ammonite zone (Paul et al. 1994, Gale 1995, Mitchell et al. 1996, Voigt et al. 2004, Jarvis et al. 2006, Joo and Sageman 2014) and near the base of nannofossil Zone UC3 (Gambacorta et al. 2015) it is likely that the FAD lies within the upper *dixoni* ammonite zone.

4.3. *Thalmanninella reicheli* and *Thalmanninella micheli*

The FAD of *T. reicheli* (Mornod) has been used to define the base of the (essentially) middle Cenomanian *reicheli* Zone since Bolli's original scheme in 1966 (see Fig. 1). However, *T. reicheli* is very rare or largely absent in sections outside the Neotethys realm, and even within it can be rare or specimens can be fragmentary (Hart et al. 1989, Gilardoni 2017, Petrizzo and Gilardoni 2020, Dr Haydon Bailey 2021, pers. comm.). For example, at the Bottaccione section at Gubbio, Premoli Silva and Sliter (1995) record *T. reicheli* as "rare" in only two samples. Moreover, to the authors' knowledge, *T. reicheli* has never been reported from the Western Interior Basin.

There is also much potential for confusion with very similar taxa such as *Thalmanninella micheli* (Sacal and Debourle) which ranges lower than *T. reicheli* and

which can therefore result in the incorrect recognition of the *reicheli* Zone (Caron and Spezzaferri 2006, Dr. Brian Huber 2021, pers. comm). See also similarities between images of these two species in Huber et al. (2016 – 'Mikrotax') and *Thalmanninella deeckei* (Franke) (Gilardoni 2017).

The *T. reicheli* Zone (i. e., as defined by the total range of *T. reicheli*) is associated with the two MCE 1 $\delta^{13}C$ isotope peaks as confirmed by Gale (1995) and Ando et al. (2009).

4.4. *Thalmanninella deeckei*

Thalmanninella deeckei (Franke) is often confused with *T. reicheli* and *T. greenhornensis* (Pessagno 1967, Ando and Huber 2007, Prof. Brian Huber 2021, pers. comm.) although its range should not overlap with the former. *T. deeckei* and *T. reicheli* have similar plano-convex lateral profiles and umbilical and spiral side features, differing only by umbilical side sutures (Petrizzo and Gilardoni 2020) which would be very difficult to distinguish in thin-section. Its LAD event is regarded as biostratigraphically reliable (Falzoni et al. 2018).

4.5. *Rotalipora cushmani*

Potential confusion with *Rotalipora montsalvensis* (Mornod), its immediate ancestor, exists resulting in possible older placement of the base of the *cushmani* zone (e. g., Georgescu 2017, who regards *R. montsal-vensis* to fall within the variability of *R. cushmani* and thus a junior synonym). Respective morphological differences between the two are discussed by Gonzalez-Donoso et al. (2007), Sorman et al. (2016) and Gilardoni (2017) (see also Caron and Spezzaferri 2006). There are also intermediate forms between the two and defining the exact transition point between the two species can be subjective and difficult. The question of potential synonymy (Georgescu 2017) remains unresolved because – intermediate forms notwithstanding – 'end member' morphology is quite distinct. Results from a quantitative biometric approach to define species boundaries between these two taxa appear equivocal (Sorman et al. 2016) and qualitative measurements such as the degree of biconvexity, the angularity of the periphery and strength of the keel, the nature (raised cf. flush or depressed) of spiral side sutures and umbilical side ornamentation are all key (but subjective) features for identification (see also Appendix A).

The correct identification in samples of *R. cushmani* and *R. montsalvensis* (if the two species are not synonymised) perhaps encapsulates the general challenges encountered in Cenomanian planktonic foram biostratigaphy. If such difficulties arise in speciating 3-dimensional, loose specimens, then speciating specimens in thin-section will be considerably harder (see below for the discussion on results from the Bottaccione section at Gubbio, Italy). This particular challenge (and others mentioned herein) is out-with the scope of this paper and would benefit from a full 'collegiate' review of Cenomanian planktonic foraminiferal taxonomy.

'Atypical' forms of *R. cushmani* have also been identified (e. g., Desmares et al. 2007, Falzoni et al. 2018). These have been found in levels both within the range of, and above the extinction of *R. cushmani* (*sensu stricto*) which is normally found around peak A or between peaks A and B of the $\delta^{13}C$ curve for OAE2 (Falzoni et al. 2018). Desmares et al. (2007) regards these atypical forms as attributed to the "…degradation of the species at global scale in response to the expansion of the oxygen minimum zone" (i. e., the onset of OAE2). These atypical forms are characterised by a weaker keel development compared to *R. cushmani s.s.*, but not so weak as to lose the keel almost entirely as in the genus *Anaticinella* (the two species of which appear to have arisen separately from *R. cushmani* and *T. greenhornensis* – see below) perhaps in response to the same environmental pressures which favoured species that could inhabit shallower waters, and were thus facilitated in doing so by the reduction/loss of the keel. Nevertheless, neither keeled, reduced-keeled or non-keeled rotaliporids survived the environmental catastrophe that was OAE2, and all became extinct at this time.

The FAD of *R. cushmani* is slightly above the so-called 'P/B Break' in the UK (Jarvis et al. 2006) – a level where the proportion of planktonic forams dramatically increases in assemblages and also a $\delta^{13}C$ event – but occurs slightly earlier in Germany (Meyer 1990 although see also Erbacher et al. 2020). The 'P/B Break' $\delta^{13}C$ event is calibrated to the middle part of the *rhotomagense* ammonite zone in several UK localities (Jarvis et al. 2006). Eldrett et al. (2015) assigned ages of this FAD event in the Eagle Ford Formation, WIB, based on orbital forcing-calibration of 96.06 and 96.20 Ma (both with error bars between 0.12 and 0.17) and 95.23 and 95.30 Ma (errors between 0.12 and 0.17) for the FAD of consistent records, placing both events above the MCE.

Falzoni et al. (2018) also regard the Last Appearance Datum (LAD) of *R. cushmani* as diachronous from south to north in the Western Interior Basin, citing shallower water refuges which favoured the survival in certain areas of the last representatives of this species.

4.6. *Anaticinella*

Common in – but not restricted to – the WIB (see Demares et al. 2007 for references), the two species of *Anaticinella* (*A. multiloculata* (Morrow) and *A. planoconvexa* (Longoria)) descended from *T. greenhornensis* and *R. cushmani* respectively by (i) the loss of ornamental elements and keel as possible adaptations to changing environmental conditions such as more anoxic conditions at depth (Ando and Huber 2007, Caron et al. 2006) and thus are ecophenotypic, Chor (ii) by a slower growth rate (Desmares et al. 2003, Desmares et al. 2007). However, Gonzalez-Donoso et al. (2007) considered *Anaticinella* specimens to be simply extreme variants of the latest *Thalmanninella* species and synonymised the genus with *Thalmanninella*. Caron et al. (2006) maintained the genus as separate but synonymised the two species under *A. planoconvexa*, and suggested that, if recorded, the (maximum) LAD of the genus could be an event close to the Cenomanian-Turonian boundary and which could be used to subdivide the *W. archaeocretacea* Zone. However, Falzoni et al. (2018) regarded this event as diachronous.

The genus – comprising both separate species – is maintained as separate within the Rotaliporidae by Huber et al. (2016 – 'Mikrotax') although it appears there is nothing conclusive to confirm either viewpoint and a thorough revision of this taxonomic group is necessary. On Fig. 2 the FAD and LAD events are shown for the genus (*Anaticinella* spp.).

4.7. *Helvetoglobotruncana helvetica* and *Helvetoglobotruncana praehelvetica*

Although the FAD of *H. helvetica* (Bolli) occurs within the (lower) Turonian its ancestor's FAD (i. e., that of *H. praehelvetica* (Trujillo)) occurs within the upper Cenomanian. Confusion between the two species can result in a low placement of the base of the *H. helvetica* Zone, thus reducing the duration of the *W. archaeocretacea* Interval Zone (see Desmares et al. 2007) and the incorrect placement of the Cenomanian-Turonian boundary. Huber and Petrizzo (2014) revised and clarified the taxonomic differences between the two species and regarded Desmares et al.'s identifications of *H. helvetica* in the Turonian GSSP section at Pueblo, Colorado (with a concomitant lowering of the base of the *H. helvetica* Zone), as *H. praehelvetica*. They also introduced a note of caution on the reliability of zonal placement stating that *H. helvetica* is generally very rare in the lower part of its stratigraphic range and increasingly rare to absent in higher latitudes or more nearshore environments.

A very detailed study by Falzoni et al. (2018), determined the order and reliability of planktonic foraminifera bioevents across the Cenomanian-Turonian boundary from the *cushmani* to *helvetica* Zones in the WIB. They concluded the FADs of both *H. helvetica* and *H. praehelvetica* were unreliable because of taxonomic uncertainties, subjective species concepts and transitional forms between them and their ancestral species. See also the review of the position and boundaries of the *helvetica* Zone with respect to δ^{13}C isotope curves by Wendler (2013) (and discussion below) which shows that the base of the zone occurs most frequently within the *nodosoides* ammonite zone (near the 'C2' δ^{13}C event just beneath 'Lulworth' – see Fig. 2 herein), but can occur as deep as around the 'Holywell' δ^{13}C event in some sections (possibly even lower at Gubbio) and even lower – within OAE2 – at Eastbourne, UK.

As a consequence, the base of the *H. helvetica* zone is shown as a diagonal line in Fig. 2 herein.

5.   Biozonation and calibration of zones to the Geological Timescale

Calibration of Cenomanian planktonic foraminiferal biozones to the standard chronostratigraphy and timescale has, as with many fossil groups in many parts of the geological column, been variable. There are many reasons for this (see Simmons and Bidgood 2022, for a general discussion). For example, the Cenomanian planktonic foraminiferal biozone calibration in GTS2020 (Gale et al. 2020 after Coccioni and Premoli Silva 2015) contrasts with that of many other interpretations.

Because most biozones are defined based on an agreed order of the inception (FAD) or extinction (LAD) events of so-called 'marker species', it is important that confidence in that order is high. It follows that the unambiguous definitions of taxa

and subsequent identification of marker species in samples is necessary to establish that order and before biozones can be assigned to intervals of rock. Discussions above show that this has not always been possible for the Cenomanian (and for other periods in deep time).

The range chart shown in Fig. 2 shows what we believe (notwithstanding the above caveats) to be the correct *order* of Cenomanian planktonic foraminiferal events based on the references studied. However, some of these events can be calibrated to the GTS better than others. For example, the worldwide identification of the *T. reicheli* Zone – though succinctly enough defined – is very difficult because of the scarcity and limited distribution of the marker species itself.

Resolving discrepancies between events may be possible through the use of a non-biostratigraphic proxy, for example, carbon isotopes. Whilst a C-isotope curve is not unique, and that some named excursion events (see Fig. 2) may not be truly global and therefore not discernible everywhere, it has the potential to independently calibrate biostratigraphic events in a variety of facies – a Rosetta Stone. It can be key to unravelling the chronostratigraphic calibration of biostratigraphic events in various sections, provided the fossil identifications are correct. Luber et al. (2019) applied this reasoning in their assessment of Aptian biostratigraphy in Morocco.

For the Cenomanian, the works of Scholle and Arthur (1980), Jenkyns (1985), Paul et al. (1994), Mitchell et al. (1996), Coccioni and Galeotti (2003), Jarvis et al. (2006), Wilmsen (2007), Gale et al. (2011), Wendler (2013), Joo and Sageman (2014), Gambacorta et al. (2015), and Cramer and Jarvis (2020), provide useful summaries of carbon isotope stratigraphy. The names of the major and minor excursion events identified are shown in Fig. 2, although it should be noted that some minor events have not been confidently recorded outside Europe (Jarvis et al. 2006). Carbon isotope stratigraphy is of increasing importance in calibrating Cenomanian planktonic foraminiferal biostratigraphy, but as the following discussion highlights, it is not without controversy.

The GTS2020 (Gale et al. 2020) Cenomanian planktonic foraminiferal biozonation scheme is based on the work of Coccioni and Premoli Silva (2015), which in turn followed that of Premoli Silva and Sliter (1995) using the Bottaccione Gorge section at Gubbio, Italy as a standard. Strikingly in this interpretation, the *reicheli* Zone is placed well down in the lower Cenomanian (within the uppermost part of the Albian-

Cenomanian Boundary Event (ACBE) on the δ^{13}C isotope curve: Coccioni and Premoli Silva 2015, fig. 2) whereas previously it has had a general middle Cenomanian placement (Robaszynski and Caron 1995, see Fig. 1). In GTS2020 (Gale et al. 2020, fig. 27.9) the δ^{13}C curve is not shown but the *reicheli* Zone is shown to lie within a sequence of 5 *Neogastroplites* ammonite zones of the Western Interior ammonite zonation scheme (Cobban et al. 2006) and the *Inoceramus crippsi* inoceramid zone (Walaszczyk and Cobban 2016), both calibrated to within the lower Cenomanian interval. Thus the bulk of the Cenomanian stage at Gubbio in the interpretations of Premoli Silva and Sliter (1995), Coccioni and Galeotti (2003), Coccioni and Premoli Silva (2015) and Gale et al. (2020) is occupied by the *cushmani* Zone (Fig. 3). This arrangement was first commented on by Jarvis et al. (2006) who stated (p. 595) "This major discrepancy in the relative positions of the *R. cushmani* and *R. reicheli* Zones [at Gubbio] requires urgent investigation."

The Gubbio section is renowned as a world-class exposure of Upper Cretaceous sediments which has been intensively studied and includes good carbon-isotope data throughout (Voigt et al. 2012, Sprovieri et al. 2013). The Cenomanian is expressed in the top c.50 metres of the Scaglia Bianca Formation and includes clear Carbon isotope signatures (δ^{13}C) for the Albian-Cenomanian Boundary Event (ACBE) a.k.a. OAE 1d, Mid Cenomanian Excursion events 1 and 2 (MCE I and MCE II), and the Cenomanian-Turonian Boundary Event (CTBE) a.k.a. OAE2.

According to Coccioni and Premoli Silva (2015), at Gubbio the *globotruncanoides* Zone is placed entirely within the upper part of the ACBE, the *reicheli* Zone at the top of the ACBE with the FAD of *R. cushmani* occurring only 1 metre or so above this (Coccioni and Premoli Silva 2015, fig. 2). A parallel study on the calcareous nannofossils (Tremolada 2002) yields only a very generalised nannofossil biostratigraphy with a boundary between two intervals – BC27-UC0 and UC1-UC5 – being placed just above the top of the *reicheli* Zone (Fig. 2). The base of the UC1 zone is most recently (GTS2020) calibrated as very close to the base of the Cenomanian (i. e., base *globotruncanoides* zone within the *briacensis* ammonite subzone) in the Tethyan realm, based on data from ODP Leg 171B where the FAD of nannofossil *Corolithion kennedyi* is recorded 2 precession cycles (0.05 myr) above the FAD of *T. globotruncanoides*. This is lower than in the lower *carcitanense* ammonite subzone where it was placed by Burnett (1998). On the other
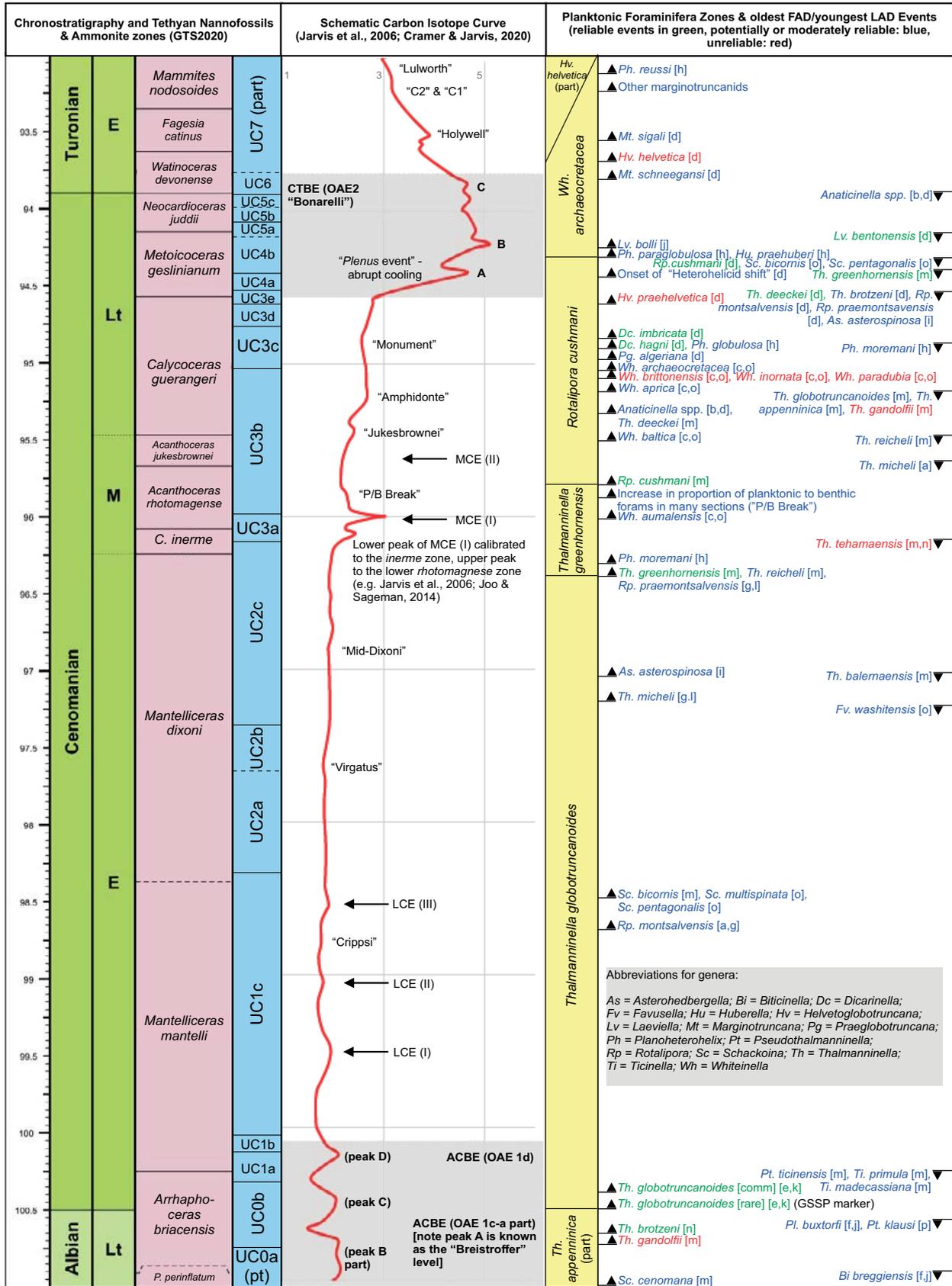
Chronostratigraphy and Tethyan Nannofossils & Ammonite zones (GTS2020)	Schematic Carbon Isotope Curve (Jarvis et al., 2006; Cramer & Jarvis, 2020)	Planktonic Foraminifera Zones & oldest FAD/youngest LAD Events (reliable events in green, potentially or moderately reliable: blue, unreliable: red)

Chronostratigraphy and Tethyan Nannofossils & Ammonite zones (GTS2020)

Turonian — E
- Mammites nodosoides — UC7 (part)
- Fagesia catinus
- Watinoceras devonense — UC6

Cenomanian — Lt
- Neocardioceras juddii — UC5c / UC5b / UC5a
- Metoicoceras geslinianum — UC4b / UC4a
- (Lt) UC3e / UC3d
- Calycoceras guerangeri — UC3c
- Acanthoceras jukesbrownei — UC3b
- Acanthoceras rhotomagense (M)
- C. inerme — UC3a

- Mantelliceras dixoni — UC2c / UC2b / UC2a
- (E)

- Mantelliceras mantelli — UC1c

- Arrhaphoceras briacensis — UC1b / UC1a / UC0b / UC0a (pt)
- P. perinflatum

Albian — Lt

Numeric scale (left): 93.5, 94, 94.5, 95, 95.5, 96, 96.5, 97, 97.5, 98, 98.5, 99, 99.5, 100, 100.5

Schematic Carbon Isotope Curve

Scale: 1 ... 3 ... 5

- "Lulworth"
- "C2" & "C1"
- "Holywell"
- C — CTBE (OAE2 "Bonarelli")
- B
- "Plenus event" - abrupt cooling
- A
- "Monument"
- "Amphidonte"
- "Jukesbrownei"
- ← MCE (II)
- "P/B Break"
- ← MCE (I)
- Lower peak of MCE (I) calibrated to the *inerme* zone, upper peak to the lower *rhotomagense* zone (e.g. Jarvis et al., 2006; Joo & Sageman, 2014)
- "Mid-Dixoni"
- "Virgatus"
- ← LCE (III)
- "Crippsi"
- ← LCE (II)
- ← LCE (I)
- (peak D) — ACBE (OAE 1d)
- (peak C)
- ACBE (OAE 1c-a part) [note peak A is known as the "Breistroffer" level]
- (peak B part)

Planktonic Foraminifera Zones & oldest FAD/youngest LAD Events

Zones (right column, yellow):
- Hv. helvetica (part)
- Wh. archaeocretacea
- Rotalipora cushmani
- Thalmanninella greenhornensis
- Thalmanninella globotruncanoides
- Th. appenninica (part)

Events:
- ▲ Ph. reussi [h]
- ▲ Other marginotruncanids
- ▲ Mt. sigali [d]
- Hv. helvetica [d]
- ▲ Mt. schneegansi [d]
- Anaticinella spp. [b,d] ▼
- ▲ Lv. bolli [j]   Lv. bentonensis [d] ▼
- ▲ Ph. paraglobulosa [h], Hu. praehuberi [h]
- Rp.cushmani [d], Sc. bicornis [o], Sc. pentagonalis [o] ▼
- ▲ Onset of "Heterohelicid shift" [d]   Th. greenhornensis [m] ▼
- Hv. praehelvetica [d]   Th. deeckei [d], Th. brotzeni [d], Rp. montsalvensis [d], Rp. praemontsalvensis [d], As. asterospinosa [i] ▼
- ▲ Dc. imbricata [d]
- ▲ Dc. hagni [d], Ph. globulosa [h]   Ph. moremani [h] ▼
- ▲ Pg. algeriana [d]
- ▲ Wh. archaeocretacea [c,o], Wh. inornata [c,o], Wh. paradubia [c,o]
- ▲ Wh. brittonensis [c,o]
- ▲ Wh. aprica [c,o]   Th. globotruncanoides [m], Th. appenninica [m], Th. gandolfii [m] ▼
- ▲ Anaticinella spp. [b,d], Th. deeckei [m]
- ▲ Wh. baltica [c,o]   Th. reicheli [m] ▼
- Th. micheli [a] ▼
- ▲ Rp. cushmani [m]
- ▲ Increase in proportion of planktonic to benthic forams in many sections ("P/B Break")
- ▲ Wh. aumalensis [c,o]   Th. tehamaensis [m,n] ▼
- ▲ Ph. moremani [h]
- ▲ Th. greenhornensis [m], Th. reicheli [m], Rp. praemontsalvensis [g,l]
- ▲ As. asterospinosa [i]   Th. balernaensis [m] ▼
- ▲ Th. micheli [g.l]   Fv. washitensis [o] ▼
- ▲ Sc. bicornis [m], Sc. multispinata [o], Sc. pentagonalis [o]
- ▲ Rp. montsalvensis [a,g]

Abbreviations for genera:
As = Asterohedbergella; Bi = Biticinella; Dc = Dicarinella; Fv = Favusella; Hu = Huberella; Hv = Helvetoglobotruncana; Lv = Laeviella; Mt = Marginotruncana; Pg = Praeglobotruncana; Ph = Planoheterohelix; Pt = Pseudothalmanninella; Rp = Rotalipora; Sc = Schackoina; Th = Thalmanninella; Ti = Ticinella; Wh = Whiteinella

- Pt. ticinensis [m], Ti. primula [m] ▼
- ▲ Th. globotruncanoides [comm] [e,k]   Ti. madecassiana [m]
- ▲ Th. globotruncanoides [rare] [e,k] (GSSP marker)
- ▲ Th. brotzeni [n]   Pl. buxtorfi [f,j], Pt. klausi [p] ▼
- Th. gandolfii [m]
- ▲ Sc. cenomana [m]   Bi breggiensis [f,j] ▼

Fig. 2. Summary biozonation and range events (FAD and LAD) for Cenomanian planktonic foraminifera and the schematic $\delta^{13}C$ isotope curve data calibrated to the GTS2020 timescale and Tethyan ammonite zones. Caution – not all named $\delta^{13}C$ signals or planktonic foram events will be recorded in every section. Range limits are the verified *maxima* recorded in the literature. References for labelled events are: a – Caron & Spezzaferri (2006); b – Caron et al. (2006); c – Falzoni et al. (2016); d – Falzoni et al. (2018); e – Gale et al. (2020); f – Gilardoni (2017); g – Gonzalez-Donoso et al. (2007); h – Haynes et al. (2015); i – Huber et al. (2016 – 'Mikrotax'); j – Huber et al. (2022); k – Kennedy et al. (2004); l – Lipson-Benitah (2008); m – Petrizzo & Gilardoni (2020); n – Petrizzo et al. (2015); o – Premoli Silva & Verga (2004); p – Spezzaferri & Caron (2008). Timescale is GTS2020 generated by Timescale Creator (ver. 8.0).

hand, within the *text* of the paper, Coccioni and Premoli Silva (2015) describe the chronostratigraphic ages of the *globotruncanoides*, *reicheli* and *cushmani* Zones as lower Cenomanian, middle Cenomanian, and late middle to uppermost Cenomanian, respectively – ages much more akin to the 'classic' zonal arrangement. However, the position of the zonal defining events observed by Premoli Silva and Sliter (1995) and Coccioni and Premoli Silva (2015) – the latter with respect to the $\delta^{13}C$ curve – tells a different story. What is the reason for this major discrepancy?

We have not examined the original Gubbio material but note that none of the stratigraphically important Cenomanian taxa are illustrated in Coccioni and Premoli Silva (2015). Illustrations can be found, however, in the earlier publication on the Gubbio section by Premoli Silva and Sliter (1995). These are all of specimens in thin-section, identification by which has taxonomic and identification challenges of its own (see Schlagintweit and Simmons (2022) for comparable views in larger benthic foraminifera). No liberated, 3D specimens were studied.

The single illustration of *T. reicheli*, the total range of which at Gubbio defines the nominal biozone (Premoli Silva and Sliter 1995, plate 8, fig. 6 – reproduced in Fig. 3 herein), is highly uncertain at best and cannot be said to confirm the identification. Without reproducing the entire original description (Mornod 1950), characteristics of *T. reicheli* include a flat or concave spiral surface and a plano-convex umbilical surface with a wide umbilicus. Caron and Spezzaferri (2006) – who redescribed and re-illu-

strated Mornod's holotypes – describe *T. reicheli* as having a "distinct planoconvex, more or less cylindrical profile. The spiral side is flat to slightly concave [easily visible on the holotype], the umbilical side is highly convex". None of these features can be observed in the illustrated specimen, nor (given the single thin-section illustration) additional but critical features such as number of chambers, nature of the keel, nor nature of the aperture and its accessory structures. It does not appear comparable with illustrations of the species in other repositories such as Mikrotax (Huber et al. 2016) and therefore its identification at Gubbio – and the consequent placement of the *T. reicheli* Zone – must be questioned. In fact, it is difficult to make any meaningful identification of the taxon actually represented by Premoli Silva and Sliter 1995, plate 8, fig. 6.

Illustrations of two other important taxa – *T. greenhornensis* and *R. cushmani* – confirm the identifications (within the limits attainable by thin-section discrimination) but these are taken from specimens considerably higher in the Gubbio section than their lowest recorded limits. Both taxa have their *recorded* FAD events at the same level (68.9m) but their lowest *illustrated* levels are 18.6 m and 25.1 m higher respectively (Fig. 3). Thus the identity of the specimens actually used to position the lower boundary of the *R. cushmani* Zone at Gubbio cannot be verified and therefore the placement of this boundary is also unconfirmed. Premoli Silva and Sliter (1995) *may* have used a broad species concept when identifying *R. cushmani* (perhaps including concepts expanded upon later by Georgescu 2017). As there are many intermediate forms between *R. cushmani* and its ancestor, *R. montsalvensis*, it is possible that these intermediates may have been included in their concept of *R. cushmani*, thus lowering the apparent FAD and base of the nominate zone (Prof. Maria Rose Petrizzo 2021, pers. comm.). Note that some recent workers (e. g., Georgescu 2017) have even included unequivocal specimens of *R. montsalvensis* within their concept of *R. cushmani*.

In summary, uncertainty as to the identification of the key taxa at the critical levels in the Gubbio section as documented by Premoli-Silva and Sliter (1995) and Coccioni and Premoli Silva (2015) precludes confirmation of the somewhat radical chronostratigraphic calibration of Cenomanian planktonic foraminiferal biostratigraphy as documented by Gale et al. (2020).

The *prima facie* planktonic foraminiferal biostratigraphy at Gubbio appears to be contradicted almost

Fig. 3. Biostratigraphic summary (left) of the Cenomanian Scaglia Bianca Formation at Bottaccione, Gubbio, Italy, by Premoli Silva and Sliter (1995) and Coccioni and Premoli Silva (2015, fig. 2). Positions of lowest recorded datums and lowest illustrated datums are shown of the three critical marker species; *Thalmanninella reicheli*, *T. greenhornensis* and *Rotalipora cushmani* (Premoli Silva and Sliter 1995). (Right): FAD events of *T. greenhornensis* and *R. cushmani* with respect to a Carbon isotope curve at Monte Petrano, Italy (slightly modified after Petrizzo and Gilardoni 2020, fig. 7) are also shown. An alternative and herein favoured zonation for the Gubbio section is also shown (centre).

everywhere else – including at a locality in Italy (Monte Petrano) only around 20km away from Gubbio – where the *reicheli* Zone is associated with the δ¹³C MCE I and MCE II events (notwithstanding the comments above made against the suitability of this species and identification of this zone) (Petrizzo and Gilardoni 2020). In addition, the FADs of *T. greenhornensis* and *R. cushmani* are always recorded respectively just below and just above the MCE δ¹³C events (Paul et al. 1994, Ando et al. 2009, Gertsch et al. 2010, Petrizzo and Gilardoni 2020;) and the LAD of *R. cushmani* occurring in the lower part of the CTBE (=OAE2) (Falzoni et al. 2018).

The alternative *suggested* placements for the base of the *R. cushmani* and *T. greenhornensis* zones at Gubbio based on illustrated specimens of those respective species rather than the lowest recorded (but unillustrated) occurrences and the removal of the *T. reicheli* zone based on no apparent verifiable illustration (Fig. 3) seem to be more reasonably in line with associated features on the δ¹³C curve.

Cenomanian chronostratigraphic subdivision is based on the calibrated δ¹³C curves in the respective sections (after Sprovieri et al. 2013 in the case of Gubbio) with the base of the middle Cenomanian drawn slightly below the MCE (I) event (which is calibrated to the *inerme* and lower *rhotomagense* ammonite zones; Jarvis et al. 2006) and the base of the upper Cenomanian drawn close to the '*jukesbrownei*' event (in the lowermost *guerangeri* ammonite zone).

Inconsistencies in picking the FAD of *H. helvetica* at the GSSP section for the base Turonian at Pueblo, Colorado (Kennedy et al. 2005) have also resulted in mis-calibrations. The FAD event has been variously placed in beds 86, 89, 102 and 103 at Pueblo by various authors between 1985 and 2016 (see Falzoni et al.

2018). Again, the role of 2-dimensional (thin-section) analyses compared with 3-dimentional (washed and extracted) specimens in the analyses may have been significant.

Studies elsewhere have also highlighted variable calibration between so-called 'standard' planktonic foraminiferal, nannofossil and ammonite zonations for other Cretaceous stages (e. g., the Aptian – see Luber et al. 2017, Luber et al. 2019, Bulot et al. 2022). While calibration between planktonic foraminiferal biozones and, for example, larger benthic foraminifera will always be challenging due to preferred habitat differences, cross-calibration of biozones based on other marine plankton such as nannofossils, dinoflagellates and microcrinoids should be possible. Moreover, the use of Carbon-isotope curve data provides a non-biostratigraphic proxy with which to potentially resolve discrepancies (see above).

Research papers from the Cenomanian involving the contemporaneous study of more than one fossil type from identical samples in the same section(s) are moderately common and typically involve planktonic foraminifera, nannofossils and ammonites together with (occasionally) δ¹³C data (e. g., Lowery et al. 2014, Gertsch et al. 2010, Gale et al. 1996, Bauer et al. 2001, Luciani and Cobianchi 1999, Kedzierski et al. 2012, Ando et al. 2015, Huber et al. 2017, Coccioni and Galeotti 2003, Schulze 2003, Keller et al. 2008).

Calibration data for key Cenomanian planktonic foraminifera are shown in Appendix 1.

6.   Conclusions

The biozonation scheme for Cenomanian planktonic foraminifera as shown in the latest iteration of the geological timescale, GTS2020, (Gale et al. 2020) appears to be in error with respect to the chronostratigraphic calibration of its constituent biozones. This is probably due to incorrect species concepts and identification of key forms at the key locality at Gubbio, Italy (Premoli Silva and Sliter 1995, Coccioni and Premoli Silva 2015). An alternative interpretation for that section is suggested (Fig. 3). We recommend a major collaborative review of all mid-Cretaceous planktonic foraminiferal taxonomy, evolutionary relationships and biostratigraphy following models established in the Cenozoic (e. g., Olsson 1999, Pearson et al. 2006 and Wade et al. 2018), with emphasis on the clear and unambiguous definitions and illustrations of valid taxa, calibration of biostratigraphic zonations between dif-

ferent fossil groups and integration with, for example, carbon isotope (δ^{13}C) curve data. The latter of which has the potential to provide excellent independent calibration and correlation potential.

Until this occurs, we consider that the biozonation schemes of Petrizzo and Gilardoni 2020 (for the 'lower' part of the Cenomanian) and Robaszynski and Caron 1995 (for the 'upper' part of the Cenomanian) used in conjunction, are the most realistic and practical and should be adopted (Table 1).

References

Al-Husseini, M. (2018). Arabian orbital sequences. In M. Montenari (Ed.), *Stratigraphy and Timescales, Volume Three: Cyclostratigraphy and Astrochronology* (pp. 219–264). Amsterdam: Elsevier. https://doi.org/10.1016/bs.sats.2018.08.001

Alsharhan, A. S., & Scott, R. W. (2000). Hydrocarbon potential of Mesozoic carbonate platform-basin systems, U. A. E. In A. S. Alsharhan, & R. W. Scott (Eds.), *Middle East Models of Jurassic/Cretaceous Carbonate Systems. Society of Economic Paleontologists and Mineralogists Special Publication*, 69, 335–358.

Ando, A., & Huber, B. T. (2007). Taxonomic revision of the Late Cenomanian planktonic foraminifera *Rotalipora greenhornensis* (Morrow, 1934). *Journal of Foraminiferal Research*, 37(2), 160–174. https://doi.org/10.2113/gsjfr.37.2.160

Ando, A., Huber, B. T., MacLeod, K. G., & Watkins, D. K. (2015). Early Cenomanian "hot greenhouse" revealed by oxygen isotope record of exceptionally well-preserved foraminifera from Tanzania. *Paleoceanography*, 30(11), 1556–1572. https://doi.org/10.1002/2015PA002854

Ando, A., Huber, B. T., MacLeod, K. G., Ohta, T., & Khim, B.-K. (2009). Blake Nose stable isotopic evidence against the mid-Cenomanian glaciation hypothesis. *Geology*, 37 (5), 451–454. https://doi.org/10.1130/G25580A.1

Batenburg, S. J., De Vleeschouwer, D., Sprovieri, M., Hilgen, F. J., Gale, A. S., Singer, B. S., … Montanari, A. (2016). Orbital control on the timing of oceanic anoxia in the Late Cretaceous. *Climate of the Past*, 12(10), 1995–2009. https://doi.org/10.5194/cp-12-1995-2016

Bauer, J., Marzouk, A. M., Steuber, T., & Kuss, J. (2001). Lithostratigraphy and biostratigraphy of the Cenomanian–Santonian strata of Sinai, Egypt. *Cretaceous Research*, 22(4), 497–526. https://doi.org/10.1006/cres.2001.0270

Beil, S., Kuhnt, W., Holbourn, A. E., Aquit, M., Flogel, S., Chellai, E. H., & Jabour, H. (2018). New insights into Cenomanian paleoceanography and climate evolution from the Tarfaya Basin, southern Morocco. *Cretaceous Research*, 84, 451–473. https://doi.org/10.1016/j.cretres.2017.11.006

Bolli, H. M. (1966). Zonation of Cretaceous to Pliocene marine sediments based on planktonic foraminifera. *Boletin Informativo Asociacion Venezolana de Geologia. Mineria y Petroleo*, 9, 3–32.

Boulila, S., Galbrun, B., Miller, K. G., Pekar, S. F., Browning, J. V., Laskar, J., & Wright, J. (2011). On the origin of Cenozoic and Mesozoic "third-order" eustatic sequences. *Earth-Science Reviews*, 109(3-4), 94–112. https://doi.org/10.1016/j.earscirev.2011.09.003

Bromhead, A. D., van Buchem, F. S. P., Simmons, M. D., & Davies, R. B. (2022). Sequence stratigraphy, paleogeography, and petroleum plays of the Cenomanian-Turonian succession of the Arabian Plate: an updated synthesis *Journal of Petroleum Geology*, 45(2), 119–162. https://doi.org/10.1111/jpg.12810

Bulot, L., Redfern, J., Luber, T. L., Simmons, M. D., & Jeremiah, J. (2022). Back to the field: the limits of standard scales in high resolution stratigraphy. Examples from North West Africa and the Middle East. In: A. Çiner, S. Grab, E. Jaillard, D. Doronzo, A. Michard, M. Rabineau & H. I. Chamin (Eds.), *Recent Research on Geomorphology, Sedimentology, Marine Geosciences and Geochemistry. Proceedings of the 2nd Springer Conference of the Arabian Journal of Geosciences (CAJG-2), Tunisia 2019* (pp. 185–187). Springer.

Burnett, J. A. (1998). Upper Cretaceous. In P. R. Bown (Ed.), *Calcareous Nannofossil Biostratigraphy* (pp. 132–199). London: Chapman & Hall. https://doi.org/10.1007/978-94-011-4902-0_6

Caron, M. (1985). Cretaceous planktonic foraminifera. In H. M. Bolli, J. B. Saunders, & K. Perch-Nielsen (Eds.), *Plankton Stratigraphy* (pp. 17–86). Cambridge University Press.

Caron, M., & Premoli Silva, I. (2007). New description of the rotaliporid species *brotzeni* and *globotruncanoides* Sigal, 1948 based on re-examination of type material. *Rivista Italiana di Paleontologia e Stratigrafia*, 113, 525–530.

Caron, M., & Spezzaferri, S. (2006). Scanning electron microscope documentation of the lost holotypes of Mornod, 1949: *Thalmanninella reicheli* and *Rotalipora montsalvensis*. *Journal of Foraminiferal Research*, 36(4), 374–378. https://doi.org/10.2113/gsjfr.36.4.374

Caron, M., Dall'Agnolo, S., Accarie, H., Barrera, E., Kauffman, E. G., Amédro, F., & Robaszynski, F. (2006). High-

resolution stratigraphy of the Cenomanian–Turonian boundary interval at Pueblo (USA) and Wadi Bahloul (Tunisia): Stable isotope and bio-events correlation. *Geobios*, *39*(2), 171–200. https://doi.org/10.1016/j.geobios.2004.11.004

Cobban, W. A., Walaszczyk, I., Obradovich, J. D., & McKinney, K. C. (2006). A USGS zonal table for the Upper Cretaceous middle Cenomanian-Maastrichtian of the Western Interior of the United States based on ammonites, inoceramids, and radiometric ages. *U. S. Geological Survey Open-File Report*, *1250*, 1–46.

Coccioni, R., & Galeotti, S. (2003). The mid-Cenomanian Event: Prelude to OAE 2. *Palaeogeography, Palaeoclimatology, Palaeoecology*, *190*, 427–440. https://doi.org/10.1016/S0031-0182(02)00617-X

Coccioni, R., & Premoli Silva, I. (2015). Revised Upper Albian – Maastrichtian planktonic foraminiferal biostratigraphy and magnetostratigraphy of the classical Tethyan Gubbio section (Italy). *Newsletters on Stratigraphy*, *48*(1), 47–90. https://doi.org/10.1127/nos/2015/0055

Coccioni, R., Luciani, V., & Marsili, A. (2006). Cretaceous oceanic anoxic events and radially elongated chambered planktonic foraminifera: Paleoecological and paleoceanographic implications. *Palaeogeography, Palaeoclimatology, Palaeoecology*, *235*(1-3), 66–92. https://doi.org/10.1016/j.palaeo.2005.09.024

Corbett, M. J., Watkins, D. K., & Pospichal, J. J. (2014). A quantitative analysis of calcareous nannofossil bioevents of the Late Cretaceous (Late Cenomanian – Coniacian) Western Interior Seaway and their reliability in established zonation schemes. *Marine Micropaleontology*, *109*, 30–45. https://doi.org/10.1016/j.marmicro.2014.04.002

Cramer, B. D., & Jarvis, I. (2020). Carbon isotope stratigraphy. In: F. M. Gradstein, J. G. Ogg, M. D. Schmitz, & G. M. Ogg (eds.), *Geologic Time Scale 2020* (pp. 309–343). Elsevier. https://doi.org/10.1016/B978-0-12-824360-2.00011-5

Davies, A., Gréselle, B., Hunter, S. J., Baines, G., Robson, C., Haywood, A. M., Ray, D. C., Simmons, M. D., & van Buchem, F. S. P., (2020). Assessing the impact of aquifer-eustasy on short term Cretaceous sea-level. *Cretaceous Research*, *112*, article #104445: 12 pp. https://doi.org/10.1016/j.cretres.2020.104445

Desmares, D., Crognier, N., Bardin, J., Testé, M., Beaudoin, B., & Grosheny, D. (2016). A new proxy for Cretaceous paleoceanographic and paleoclimatic reconstructions: Coiling direction changes in the planktonic foraminifera *Muricohedbergella delrioensis*. *Palaeogeography, Palaeoclimatology, Palaeoecology*, *445*, 8–17. https://doi.org/10.1016/j.palaeo.2015.12.021

Desmares, D., Grosheny, D., & Beaudoin, B. (2003). Hétérochronies du développement sensu Gould chez les foraminifères planctoniques cénomaniens: Exemple de néoténie dans le bassin du Western Interior américain. *Comptes Rendus. Palévol*, *2*(6-7), 587–595. https://doi.org/10.1016/j.crpv.2003.09.012

Desmares, D., Grosheny, D., Beaudoin, B., Gardin, S., & Gauthier-Lafaye, F. (2007). High resolution stratigraphic record constrained by volcanic ash beds at the Cenomanian-Turonian boundary in the Western Interior Basin, USA. *Cretaceous Research*, *28*(4), 561–582. https://doi.org/10.1016/j.cretres.2006.08.009

Desmares, D., Testé, M., Broche, B., Tremblin, M., Gardin, S., Villier, L., … Raboeuf, P. (2019). High-resolution biostratigraphy and chemostratigraphy of the Cenomanian stratotype area (Le Mans, France). *Cretaceous Research*, *106*, 104198. https://doi.org/10.1016/j.cretres.2019.104198

Eldrett, J. S., Ma, C., Bergman, S. C., Lutz, B., Gregory, F. J., Dodsworth, P., … Kelly, A. E. (2015). An astronomically calibrated stratigraphy of the Cenomanian, Turonian and earliest Coniacian from the Cretaceous Western Interior Seaway, USA: Implications for global chronostratigraphy. *Cretaceous Research*, *56*, 316–344. https://doi.org/10.1016/j.cretres.2015.04.010

Erbacher, J., Bornemann, A., Petrizzo, M. R., & Huck, S. (2020). Chemostratigraphy and stratigraphic distribution of keeled planktonic foraminifera in the Cenomanian of the North German Basin. *ZDGG*, *171*(2), 149–161. https://doi.org/10.1127/zdgg/2020/0211

Esrafili-Dizaji, B., & Rahimpour-Bonab, H. (2019). Carbonate reservoir rocks at giant oil and gas fields in SW Iran and the adjacent offshore: A review of stratigraphic occurrence and poro-perm characteristics. *Journal of Petroleum Geology*, *42*(4), 343–370. https://doi.org/10.1111/jpg.12741

Falzoni, F., Petrizzo, M. R., Caron, M., Leckie, R. M., & Elderbak, K. (2018). Age and synchronicity of planktonic foraminiferal bioevents across the Cenomanian–Turonian boundary interval (Late Cretaceous). *Newsletters on Stratigraphy*, *51*(3), 343–380. https://doi.org/10.1127/nos/2018/0416

Falzoni, F., Petrizzo, M. R., Jenkyns, H. C., Gale, A. S., & Tsikos, H. (2016). Planktonic foraminiferal biostratigraphy and assemblage composition across the Cenomanian-Turonian boundary interval at Clot Chevalier (Vocontian Basin, SE France). *Cretaceous Research*, *59*, 69–97. https://doi.org/10.1016/j.cretres.2015.10.028

Francis, J. E., & Frakes, L. A. (1993). Cretaceous climates. *Sedimentology Review*, *1*, 17–30. https://doi.org/10.1002/9781444304534.ch2

Gale, A. S. (1995). Cyclostratigraphy and correlation of the Cenomanian stage in Western Europe. In M. R. House, & A. S. Gale (Eds.), Geological Society, London, Special Publications, *85*. *Orbital Forcing Timescales and Cyclostratigraphy* (pp. 177–197). https://doi.org/10.1144/GSL.SP.1995.085.01.11

Gale, A. S., Bown, P., Caron, M., Crampton, J., Crowhurst, S. J., Kennedy, W. J., … Wray, D. S. (2011). The uppermost Middle and Upper Albian succession at the Col de Palluel, Hautes-Alpes, France: An integrated study (ammonites, inoceramid bivalves, planktonic foraminifera, nannofossils, geochemistry, stable oxygen and carbon isotopes, cyclostratigraphy). *Cretaceous Research*, *32*(2), 59–130. https://doi.org/10.1016/j.cretres.2010.10.004

Gale, A. S., Hardenbol, J., Hathway, B., Kennedy, W. J., Young, J. R., & Phansalkar, V. (2002). Global correlation of Cenomanian (Upper Cretaceous) sequences: Evidence for Milankovitch control on sea level. *Geology*, *30*(4), 291–294. https://doi.org/10.1130/0091-7613(2002)030<0291:GCOCUC>2.0.CO;2

Gale, A. S., Jenkyns, H. C., Tsikos, H., van Breugel, Y., Sinninghe Damsté, J. S., Bottini, C., … Wray, D. S. (2019). High-resolution bio- and chemostratigraphy of an expanded record of Oceanic Anoxic Event 2 (Late Cenomanian–Early Turonian) at Clot Chevalier, near Barrême, SE France (Vocontian Basin). *Newsletters on Stratigraphy*, *52*(1), 97–129. https://doi.org/10.1127/nos/2018/0445

Gale, A. S., Kennedy, W. J., & Petrizzo, M. R. (2021). Stratigraphy of the Albian−Cenomanian boundary interval in the Agadir Basin, Morocco: Ammonites, microcrinoids, planktonic foraminifera. *Acta Geologica Polonica*, *71*(4), 453–480.

Gale, A. S., Kennedy, W. J., Burnett, J. A., Caron, M., & Kidd, B. E. (1996). The Late Albian to Early Cenomanian succession at Mont Risou near Rosans (Drôme, SE France): An integrated study (ammonites, inoceramids, planktonic foraminifera, nannofossils, oxygen and carbon isotopes). *Cretaceous Research*, *17*(5), 515–606. https://doi.org/10.1006/cres.1996.0032

Gale, A. S., Mutterlose, J., Batenburg, S., Gradstein, F. M., Agterberg, F. P., Ogg, J. G., & Petrizzo, M. R. (2020). The Cretaceous Period. In F. M. Gradstein, J. G. Ogg, M. D. Schmitz, & M. M. Ogg (Eds.)*, Geologic Time Scale 2020* (*Vol. 2*, pp. 1023–1086). Elsevier. https://doi.org/10.1016/B978-0-12-824360-2.00027-9

Gale, A. S., Voigt, S., Sageman, B. B., & Kennedy, W. J. (2008). Eustatic sea-level record for the Cenomanian (Late Cretaceous)–Extension to the Western Interior Basin, USA. *Geology*, *36*(11), 859–862. https://doi.org/10.1130/G24838A.1

Gale, A. S., Young, J. R., Shackleton, N. J., Crowhurst, S. J., & Wray, D. S. (1999). Orbital tuning of Cenomanian marly chalk successions: towards a Milankovitch timescale for the Late Cretaceous. *Philosophical Transactions of the Royal Society of London. Series A: Mathematical, Physical and Engineering Sciences*, 357(1757), 1815–1829. https://doi.org/10.1098/rsta.1999.0402

Gambacorta, G., Jenkyns, H. C., Russo, F., Tsikos, H., Wilson, P. A., Faucher, G., & Erba, E. (2015). Carbon- and oxygen-isotope records of mid-Cretaceous Tethyan pelagic sequences from the Umbria–Marche and Belluno Basins (Italy). *Newsletters on Stratigraphy*, *48*(3), 299–323. https://doi.org/10.1127/nos/2015/0066

Georgescu, M. D. (2017). Upper Cretaceous planktic foraminiferal biostratigraphy. *Studia UBB Geologia*, *61*(1), 5–20. https://doi.org/10.5038/1937-8602.61.1.1297

Gertsch, B., Adatte, T., Keller, G., Tantawy, A. A. A. M., Berner, Z., Mort, H. P., & Fleitmann, D. (2010). Middle and Late Cenomanian oceanic anoxic events in shallow and deeper shelf environments of western Morocco. *Sedimentology*, *57*(6), 1430–1462. https://doi.org/10.1111/j.1365-3091.2010.01151.x

Gilardoni, S. E. (2017). Late Albian-Cenomanian planktonic foraminiferal biostratigraphy, taxonomy and oceanographic inferences. PhD thesis, University of Milan.

Giorgioni, M., Weissert, H., Bernasconi, S. M., Hochuli, P. A., Keller, C. E., Coccioni, R., … Garcia, T. I. (2015). Paleoceanographic changes during the Albian–Cenomanian in the Tethys and North Atlantic and the onset of the Cretaceous chalk. *Global and Planetary Change*, *126*, 46–61. https://doi.org/10.1016/j.gloplacha.2015.01.005

Gonzalez-Donoso, J. M., Linares, D., & Robaszynski, F. (2007). The Rotaliporids, a polyphyletic group of Albian-Cenomanian planktonic foraminifera: Emendation of genera. *Journal of Foraminiferal Research*, *37*(2), 175–186. https://doi.org/10.2113/gsjfr.37.2.175

Gradstein, F. M., Ogg, J. G., Schmitz, M. D., & Ogg, G. M. (Eds.). (2020). *Geologic Time Scale 2020* (Vols. 1–2). Elsevier.

Hancock, J. M. (1991). Ammonite scales for the Cretaceous System. *Cretaceous Research*, *12*(3), 259–291. https://doi.org/10.1016/0195-6671(91)90037-D

Hancock, J. M. (2004). The mid-Cenomanian eustatic low. *Acta Geologica Polonica*, *54*(4), 611–627.

Haq, B. U. (2014). Cretaceous eustasy revisited. *Global and Planetary Change*, *113*, 44–58. https://doi.org/10.1016/j.gloplacha.2013.12.007

Haq, B. U., Hardenbol, J., & Vail, P. R. (1987). Chronology of fluctuating sea levels since the Triassic. *Science*, *235*(4793), 1156–1167. https://doi.org/10.1126/science.235.4793.1156

Hardenbol, J., Thierry, J., Farley, M. B., Jacquin, T., De Graciansky, P.-C., & Vail, P. R. (1998). Mesozoic and Cenozoic sequence chronostratigraphic framework of European basin. In P.-C. de Graciansky, J. Hardenbol, T. Jacquin, & P. R. Vail (Eds.), *Mesozoic and Cenozoic Sequence Stratigraphy of European Basins* (pp 3–14). Society of Economic Paleontologists and Mineralogists Special Publication No. 60.

Hart, M. B. (2007). Late Cretaceous climates and foraminiferal distribution. In M. Williams, A. M. Haywood, F. J. Gregory, & D. N. Schmidt (Eds.), *Deep-time perspectives on climate change; marrying the signal from computer models and biological proxies* (pp. 235–250). *The Micropalaeontological Society, Special Publications*. The Geological Society, London.

Hart, M. B. (2021). The mid-Cretaceous debate: Evidence from the foraminifera. *Cretaceous Research*, *128*, 104964. https://doi.org/10.1016/j.cretres.2021.104964

Hart, M. B., Bailey, H. W., Crittenden, S., Fletcher, B. N., Price, R. J., & Swiecicki, A. (1989). Cretaceous. In D. G. Jenkins, & J. W. Murray (Eds.)*, Stratigraphical Atlas of Fossil Foraminifera* (2nd ed., pp. 273–371). Ellis Horwood Ltd.

Haynes, S. J., Huber, B. T., & MacLeod, K. G. (2015). Evolution and phylogeny of Mid-Cretaceous (Albian-Coniacian) biserial planktic foraminifera. *Journal of*

Foraminiferal Research, *45*(1), 42–81. https://doi.org/ 10.2113/gsjfr.45.1.42

Höfling, R., & Scott, R. (2002). Early and Mid-Cretaceous buildups. In W. Kiessling, E. Flügel, J. Golonka (Eds.), *Phanerozoic Reef Patterns (pp. 521–548). Society of Economic Paleontologists and Mineralogists Special Publication*, *72* https://doi.org/10.2110/pec.02.72.0521

Hong, S. K., & Lee, Y. I. (2012). Evaluation of atmospheric carbon dioxide concentrations during the Cretaceous. *Earth and Planetary Science Letters*, *327–328*, 23–28. https://doi.org/10.1016/j.epsl.2012.01.014

Huang, C. (2018). Astronomical time scale for the Mesozoic. In M. Montenari (Ed.)*, Stratigraphy and Timescales, Volume Three: Cyclostratigraphy and Astrochronology* (pp. 81–150). Amsterdam: Elsevier. https://doi.org/ 10.1016/bs.sats.2018.08.005

Huber, B. T., & Petrizzo, M. R. (2014). Evolution and taxonomic study of the Cretaceous planktonic foraminifer genus *Helvetoglobotruncana*, Reiss 1957. *Journal of Foraminiferal Research*, *44*(1), 40–57. https://doi.org/ 10.2113/gsjfr.44.1.40

Huber, B. T., Petrizzo, M. R., & Falzoni, F. (2022). Taxonomy and phylogeny of Albian-Maastrichtian planispiral planktonic foraminifera traditionally assigned to *Globigerinelloides*. *Micropaleontology*, *68*(2), 117–183. https://doi.org/10.47894/mpal.68.2.01

Huber, B. T., Petrizzo, M. R., Watkins, D. K., Haynes, S. J., & MacLeod, K. G. (2017). Correlation of Turonian continental margin and deep-sea sequences in the subtropical Indian Ocean sediments by integrated planktonic foraminiferal and calcareous nannofossil biostratigraphy. *Newsletters on Stratigraphy*, *50*(2), 141–185. https:// doi.org/10.1127/nos/2017/0373

Huber, B. T., Petrizzo, M. R., Young, J. R., Falzoni, F., Gilardoni, S. E., Bown, P. R., & Wade, B. S. (eds) (2016). pforams@mikrotax website: A new online taxonomic database for planktonic foraminifera. *Micropaleontology*, *62*(6), 429–438.

Jarvis, I., Carson, G. A., Cooper, M. K. E., Hart, M. B., Leary, P. N., Tocher, B. A., … Rosenfeld, A. (1988). Microfossil assemblages and the Cenomanian-Turonian (Late Cretaceous) oceanic anoxic event. *Cretaceous Research*, *9*(1), 3–103. https://doi.org/10.1016/0195-6671(88)90003-1

Jarvis, I., Gale, A. S., Jenkyns, H. C., & Pearce, M. A. (2006). Secular variation in Late Cretaceous carbon isotopes: A new $\delta^{13}C$ carbonate reference curve for the Cenomanian-Campanian (99.6–70.6 Ma). *Geological Magazine*, *143*(5), 561–608. https://doi.org/10.1017/ S0016756806002421

Jenkyns, H. C. (1985). The early Toarcian and Cenomanian-Turonian anoxic events in Europe: Comparisons and contrasts. *Geologische Rundschau*, *74*(3), 505–518. https://doi.org/10.1007/BF01821208

Jenkyns, H. C. (2010). Geochemistry of oceanic anoxic events. *Geochemistry, Geophysics, Geosystems*, *11*(3), Q03004. https://doi.org/10.1029/2009GC002788

Johnson, C. C. (2002). The rise and fall of Rudist reefs. *American Scientist*, *90*(2), 148–153. https://doi.org/ 10.1511/2002.2.148

Johnson, C. C., Sanders, D., Kauffman, E. G., & Hay, W. W. (2002). In W. Kiessling, E. Flügel, & J. Golonka (Eds.), *Phanerozoic Reef Patterns (pp. 549–585). Society of Economic Paleontologists and Mineralogists Special Publication*, *72*.

Joo, Y. J., & Sageman, B. B. (2014). Cenomanian to Campanian carbon isotope chemostratigraphy from the Western Interior Basin, USA. *Journal of Sedimentary Research*, *84*(7), 529–542. https://doi.org/10.2110/jsr.2014 .38

Kędzierski, M., Machaniec, E., Rodriguez-Tovar, F. J., & Uchman, A. (2012). Bio-events, foraminiferal and nannofossil biostratigraphy of the Cenomanian/Turonian boundary interval in the Subsilesian Nappe, Rybie section, Polish Carpathians. *Cretaceous Research*, *35*, 181–198. https://doi.org/10.1016/j.cretres.2011.12.010

Keller, G., & Pardo, A. (2004). Disaster opportunists Guembelitrinidae – Index for environmental catastrophes. *Marine Micropaleontology*, *53*(1-2), 83–116. https://doi.org/10.1016/j.marmicro.2004.04.012

Keller, G., Adatte, T., Berner, Z., Chellai, E. H., & Stueben, D. (2008). Oceanic events and biotic effects of the Cenomanian-Turonian anoxic event, Tarfaya Basin, Morocco. *Cretaceous Research*, *29*(5–6), 976–994. https:// doi.org/10.1016/j.cretres.2008.05.020

Kennedy, W. J., & Gale, A. S. (2017). Trans-Tethyan correlation of the Lower–Middle Cenomanian boundary interval; southern England (Southerham, near Lewes, Sussex) and Douar el Khiana, northeastern Algeria. *Acta Geologica Polonica*, *67*(1), 75–108, 108ii. https://doi.org/ 10.1515/agp-2017-0005

Kennedy, W. J., Gale, A. S., Lees, J. A., & Caron, M. (2004). The Global Boundary Stratotype Section and Point (GSSP) for the base of the Cenomanian Stage, Mont Risou, Hautes-Alpes, France. *Episodes*, *27*(1), 21–32. https://doi.org/10.18814/epiiugs/2004/v27i1/003

Kennedy, W. J., Walaszczyk, I., & Cobban, W. A. (2005). The Global Boundary Stratotype Section and Point for the base of the Turonian Stage of the Cretaceous: Pueblo, Colorado, U. S. A. *Episodes*, *28*(2), 93–104.

Koch, J. T., & Brenner, R. L. (2009). Evidence for glacioeustatic control of large, rapid sea-level fluctuations during the Albian-Cenomanian: Dakota Formation, eastern margin of Western Interior Seaway, USA. *Cretaceous Research*, *30*(2), 411–423. https://doi.org/10.1016/j.cretres.2008.08.002

Kominz, M. A., Browning, J. V., Miller, K. G., Sugarman, P. J., Mizintseva, S., & Scotese, C. R. (2008). Late Cretaceous to Miocene sea-level estimates from the New Jersey and Delaware coastal plain coreholes: An error analysis. *Basin Research*, *20*(2), 211–226. https://doi.org/ 10.1111/j.1365-2117.2008.00354.x

Ladant, J.-B., & Donnadieu, Y. (2016). Palaeogeographic regulation of glacial events during the Cretaceous super-

greenhouse. *Nature Communications*, *7*(1), 12771. https://doi.org/10.1038/ncomms12771

Laugié, M., Donnadieu, Y., Ladant, J. B., Bopp, L., Ethé, C., & Raisson, F. (2021). Exploring the impact of Cenomanian paleogeography and marine gateways on oceanic oxygen. *Paleoceanography and Paleoclimatology*, *36*7, e2020PA004202. https://doi.org/10.1029/2020PA004202

Laugié, M., Donnadieu, Y., Ladant, J. B., Green, J. A., Bopp, L., & Raisson, F. (2020). Stripping back the modern to reveal the Cenomanian–Turonian climate and temperature gradient underneath. *Climate of the Past*, *16*(3), 953–971. https://doi.org/10.5194/cp-16-953-2020

Leary, P. N., Carson, G. A., Cooper, M. K. E., Hart, M. B., Horne, D., Jarvis, I., … Tocher, B. A. (1989). The biotic response to the late Cenomanian oceanic anoxic event; integrated evidence from Dover, SE England. *Journal of the Geological Society*, *146*(2), 311–317. https://doi.org/10.1144/gsjgs.146.2.0311

Leckie, R. M., Bralower, T. J., & Cashman, R. (2002). Oceanic anoxic events and plankton evolution: Biotic response to tectonic forcing during the mid-Cretaceous. *Paleoceanography*, *17*(3), 13-1–13-29. https://doi.org/10.1029/2001PA000623 https://doi.org/10.1029/2001PA000623

Lipson-Benitah, S. (2008). Phylogeny of the Middle Cretaceous (late Albian – late Cenomanian) planktonic foraminiferal genera *Parathalmanninella* nov. gen. and *Thalmanninella*. *Journal of Foraminiferal Research*, *38*(2), 183–189. https://doi.org/10.2113/gsjfr.38.2.183

Loeblich, A. R., Jr.,, & Tappan, H. (1988). *Foraminiferal General and Their Classification* (Vols. 1–2). New York: Van Nostrand Reinhold. https://doi.org/10.1007/978-1-4899-5760-3

Lowery, C. M., & Leckie, R. M. (2017). Biostratigraphy of the Cenomanian-Turonian Eagle Ford Shale of south Texas. *Journal of Foraminiferal Research*, *47*(2), 105–128. https://doi.org/10.2113/gsjfr.47.2.105

Lowery, C. M., Corbett, M. J., Leckie, R. M., Watkins, D., Romero, A. M., & Pramudito, A. (2014). Foraminiferal and nannofossil paleoecology and paleoceanography of the Cenomanian–Turonian Eagle Ford Shale of southern Texas. *Palaeogeography, Palaeoclimatology, Palaeoecology*, *413*, 49–65. https://doi.org/10.1016/j.palaeo.2014.07.025

Luber, T. L., Bulot, L. G., Redfern, J., Frau, C., Arantegui, A., & Masrour, M. (2017). Revised ammonoid biostratigraphy for the Aptian of NW Africa: Essaouira-Agadir Basin, Morocco. *Cretaceous Research*, *79*, 12–34. https://doi.org/10.1016/j.cretres.2017.06.020

Luber, T. L., Bulot, L. G., Redfern, J., Nahim, M., Jeremiah, J., Simmons, M. D., … Masrour, M. (2019). A revised chronostratigraphic framework for the Aptian of the Essaouira-Agadir Basin, a candidate type section for the NW African Atlantic Margin. *Cretaceous Research*, *93*, 292–317. https://doi.org/10.1016/j.cretres.2018.09.007

Luciani, V., & Cobianchi, M. (1999). The Bonarelli Level and other black shales in the Cenomanian-Turonian of the northeastern Dolomites (Italy): Calcareous nannofossil and foraminiferal data. *Cretaceous Research*, *20*(2), 135–167. https://doi.org/10.1006/cres.1999.0146

Marlow, L., Kendall, C. C. G., & Yose, L. A. (Eds.). (2014). AAPG Memoir: *Vol. 106. Petroleum Systems of the Tethyan Region* (pp. 1–780). https://doi.org/10.1306/M1061343

McDonough, K. J., & Cross, T. A. (1991). Late Cretaceous sea level from a paleoshoreline. *Journal of Geophysical Research*, *96*(B4), 6591–6607. https://doi.org/10.1029/91JB00281

McGowran, B. (2005). *Biostratigraphy: microfossils and geologic time*. Cambridge University Press. https://doi.org/10.1017/CBO9780511610653

Meyer, T. (1990). Biostratigraphische und sedimentologische Untersuchungen in der Planerfazies des Cenoman von Nordwestdeutschland. *Mitteilungen aus dem Geologischen Institut der Universität Hannover*, *30*, 1–114.

Meyers, S. R., Siewert, S. E., Singer, B. S., Sageman, B. B., Condon, D., Obradovich, J. D., … Sawyer, D. A. (2012). Intercalibration of radioisotopic and astrochronologic time scales for the Cenomanian-Turonian Boundary interval, Western Interior Basin, USA. *Geology*, *40*(1), 7–10. https://doi.org/10.1130/G32261.1

Miller, K. G., Sugarman, P. J., Browning, J. V., Kominz, M. A., Hernández, J. C., Olsson, R. K., … Van Sickel, W. (2003). Late Cretaceous chronology of large, rapid sea-level changes: Glacioeustasy during the greenhouse world. *Geology*, *31*(7), 585–588. https://doi.org/10.1130/0091-7613(2003)031<0585:LCCOLR>2.0.CO;2

Miller, K. G., Sugarman, P. J., Browning, J. V., Kominz, M. A., Olsson, R. K., Feigenson, M. D., & Hernandez, J. C. (2004). Upper Cretaceous sequences and sea level history, New Jersey Coastal Plain. *Geological Society of America Bulletin*, *116*(3), 368–393. https://doi.org/10.1130/B25279.1

Miller, K. G., Wright, J. D., & Browning, J. V. (2005). Visions of ice sheets in a greenhouse world. *Marine Geology*, *217*(3-4), 215–231. https://doi.org/10.1016/j.margeo.2005.02.007

Mitchell, S. F., & Carr, I. T. (1998). Foraminiferal response to mid-Cenomanian (Upper Cretaceous) palaeoceanographic events in the Anglo-Paris Basin (Northwest Europe). *Palaeogeography, Palaeoclimatology, Palaeoecology*, *137*(1-2), 103–125. https://doi.org/10.1016/S0031-0182(97)00087-4

Mitchell, S. F., Paul, C. R. C., & Gale, A. S. (1996). Carbon isotopes and sequence stratigraphy. In J. A. Howell, & J. F. Aitken (Eds.)*, High Resolution Sequence Stratigraphy: Applications and Innovations. Geological Society of London, Special Publication*, *104* (pp. 11–24).

Morel, N. (coord.) (2015). *Stratotype Cénomanien*. 384 pp.; (Patrimoine géologie 6),Paris Muséum national d'Histoire naturelle.

Morel, N., Desmares, D., & Néraudeau, D. (2017). La paléontologie du Cénomanien. *Annales de Paléontologie*, *103*. https://doi.org/10.1016/j.annpal.2017.02.002

Mornod, L. (1950). Les Globorotalides du Crétacé superieur du Montsalvens (Prealpes fribourgeoises). *Eclogae Geologicae Helvetiae*, 42(2), 573–595.

Nederbragt, A. J. (1991). Late Cretaceous biostratigraphy and development of Heterohelicidae (planktic foraminifera). *Micropaleontology*, 37(4), 329–372. https://doi.org/10.2307/1485910

Obradovich, J. D. (1993). A Cretaceous time scale. In W. G. E. Caldwell, & E. G. Kauffman (Eds.), Geological Association of Canada Special Paper: Vol:39. *Evolution of the Western Interior Basin* (pp. 379–396).

Obradovich, J. D., Matsumoto, T., Nishida, T., & Inoue, Y. (2002). Integrated biostratigraphic and radiometric scale on the Lower Cenomanian (Cretaceous) of Hokkaido, Japan. *Proceedings of the Japan Academy. Series B, Physical and Biological Sciences*, 78(6), 149–153. https://doi.org/10.2183/pjab.78.149

O'Brien, C. L., Robinson, S. A., Pancost, R. D., Sinninghe Damsté, J. S., Schouten, S., Lunt, D. J., … Wrobel, N. E. (2017). Cretaceous sea-surface temperature evolution: Constraints from TEX86 and planktonic foraminiferal oxygen isotopes. *Earth-Science Reviews*, 172, 224–247. https://doi.org/10.1016/j.earscirev.2017.07.012

Ogg, J. G., & Hinnov, L. A. (2012). Cretaceous. In F. M. Gradstein, J. G. Ogg, M. D. Schmitz, & G. M. Ogg (Eds.), *The Geologic Time Scale 2012* (*Vol. 2*, pp. 793–853). Elsevier. https://doi.org/10.1016/B978-0-444-59425-9.00027-5

Ogg, J. G., Agterberg, F. P., & Gradstein, F. M. (2004). The Cretaceous Period. In F. M. Gradstein, J. G. Ogg, & A. Smith (Eds.), *A Geologic Time Scale 2004* (pp. 344–383). Cambridge University Press.

Ogg, J. G., Ogg, G., & Gradstein, F. M. (2008). *The Concise Geologic Time Scale*. Cambridge University Press.

Ogg, J. G., Ogg, G., & Gradstein, F. M. (2016). *A Concise Geologic Time Scale 2016*. Elsevier.

Olsson, R. K., Berggren, W. A., Hemleben, C., & Huber, B. T. (1999). *Atlas of Paleocene Planktonic Foraminifera*. Washington, DC: Smithsonian Institution Press. https://doi.org/10.5479/si.00810266.85.1

Paul, C. R. C., Mitchell, S. F., Marshall, J. D., Leafy, P. N., Gale, A. S., Duane, A. M., & Ditchfield, P. W. (1994). Palaeoceanographic events in the middle Cenomanian of Northwest Europe. *Cretaceous Research*, 15(6), 707–738. https://doi.org/10.1006/cres.1994.1039

Pearson, P. N. (1998). Evolutionary concepts in biostratigraphy. In P. Doyle, & M. R. Bennett (Eds.), *Unlocking the Stratigraphic Record* (pp. 123–144). John Wiley and Sons.

Pearson, P. N., Olsson, R. K., Huber, B. T., Hemleben, C., & Berggren, W. A. ((Eds.))(2006). Atlas of Eocene Planktonic Foraminifera. *Cushman Foundation for Foraminiferal Research. Special Publication*, 41.

Pessagno, E. A. (1967). Upper Cretaceous planktonic foraminifera from the Western Gulf Coastal Plain. *Palaeontographica Americana*, 5, 259–441.

Petrizzo, M. R., & Gilardoni, S. E. (2020). Planktonic foraminiferal biostratigraphy of Late Albian-Cenomanian pelagic sequences from the Umbria-Marche Basin (Central Italy) and the Mazagan Plateau (Northeast Atlantic Ocean). *Rivista Italiana di Paleontologia e Stratigrafia*, 126(3), 865–904.

Petrizzo, M. R., & Huber, B. T. (2006). Biostratigraphy and taxonomy of Late Albian planktonic foraminifera from ODP leg 171B (western North Atlantic Ocean). *Journal of Foraminiferal Research*, 36(2), 166–190. https://doi.org/10.2113/36.2.166

Petrizzo, M. R., Caron, M., & Premoli Silva, I. (2015). Remarks on the identification of the Albian/Cenomanian boundary and taxonomic clarification of the planktonic foraminifera index species *globotruncanoides*, *brotzen*i and *tehamaensis*. *Geological Magazine*, 152(3), 521–536. https://doi.org/10.1017/S0016756814000478

Petrizzo, M. R., Watkins, D. K., MacLeod, K. G., Hasegawa, T., Huber, B. T., Batenburg, S. J., & Kato, T. (2021). Exploring the paleoceanographic changes registered by planktonic foraminifera across the Cenomanian-Turonian boundary interval and Oceanic Anoxic Event 2 at southern high latitudes in the Mentelle Basin (SE Indian Ocean). *Global and Planetary Change*, 206, 103595. https://doi.org/10.1016/j.gloplacha.2021.103595

Philip, J. M., & Airaud-Crumiere, C. (1991). The demise of the rudist-bearing carbonate platforms at the Cenomanian/Turonian boundary: A global control. *Coral Reefs*, 10(2), 115–125. https://doi.org/10.1007/BF00571829

Plint, A. G., & Kreitner, M. A. (2007). Extensive thin sequences spanning Cretaceous foredeep suggest high-frequency eustatic control: late Cenomanian, Western Canada foreland basin. *Geology*, 35(8), 735–738. https://doi.org/10.1130/G23662A.1

Postuma, J. (1971). *Manual of Planktonic Foraminifera*. Amsterdam: Elsevier.

Premoli Silva, I., & Sliter, W. V. (1995). Cretaceous planktonic foraminiferal biostratigraphy and evolutionary trends from the Bottaccione section, Gubbio, Italy. *Palaeontographia Italica*, 82, 1–89.

Premoli Silva, I., & Verga, D. (2004). *Practical Manual of Cretaceous Planktonic Foraminifera*. In Verga and Rettori (eds), International School on Planktonic Foraminifera, 3° Course: Cretaceous. Universities of Perugia and Milan Tipografia Pontefelcino, Perugia (Italy).

Ray, D. C., van Buchem, F. S. P., Baines, G., Davies, A., Gréselle, B., Simmons, M. D., & Robson, C. (2019). The magnitude and cause of short-term eustatic Cretaceous sea-level change: a synthesis. *Earth-Science Reviews*, 197, article #102901: 20 pp. https://doi.org/10.1016/j.earscirev.2019.102901

Rineau, V., Floquet, M., Villier, L., Léonide, P., Blénet, A., & Mfere, A. P. A. (2021). Ecological successions of rudist communities: A sedimentological and palaeoecological analysis of upper Cenomanian rudist assemblages from the South-Provence Carbonate Platform (SE France). *Sedimentary Geology*, 424, 105964. https://doi.org/10.1016/j.sedgeo.2021.105964

Robaszynski, F., & Caron, M. (1995). Foraminifères planctoniques du Crétacé: Commentaire de la zonation Europe-Méditerranée. *Bulletin de la Société Géologique de France*, 6, 681–692.

Robaszynski, F., & Caron, M. (Eds.) & European Working Group on Planktonic Foraminifera (1979). *Atlas of Mid Cretaceous planktonic foraminifera (Boreal Sea and Tethys). Parts 1–2*. Cahiers de Micropaléontologie, 1–366.

Robaszynski, F., Amédro, F., González-Donoso, J. M., & Linares, D. (2008). The Albian (Vraconian)–Cenomanian boundary at the western Tethyan margin (Central Tunisia and southeastern France). *Bulletin de la Société Géologique de France*, 179(3), 245–266. https://doi.org/10.2113/gssgfbull.179.3.245

Robaszynski, F., Caron, M., Amédro, F., Dupuis, C., Hardenbol, J., González-Donoso, J. M., … Gartner, S. (1993). Le Cénomanien de la region de Kalaat Senan (Tunisie Centrale): Litho-biostratigraphie et interpretation séquentielle. *Revue de Paléobiologie*, 12, 351–505.

Robaszynski, F., Caron, M., Dupuis, C., Amédro, F., González-Donoso, J. M., Linares, D., … Deloffre, R. (1990). A tentative integrated stratigraphy in the Turonian of Central Tunisia: Formations, zones and sequential stratigraphy in the Kalaat Senan area. *Bulletin des Centres de Recherches Exploration-Production Elf-Aquitaine*, 14(1), 213–384.

Robaszynski, F., Gale, A., Juignet, P., Amédro, F., & Hardenbol, J. (1998). Sequence Stratigraphy in the Upper Cretaceous series of the Anglo-Paris Basin: exemplified by the Cenomanian stage. In P.-C. de Graciansky, J. Hardenbol, T. Jacquin, & P. R. Vail (Eds.), SEPM Special Publication: Vol. 60. *Mesozoic-Cenozoic Sequence Stratigraphy of European Basins* (pp. 363–386).

Robaszynski, F., Hardenbol, J., Caron, M., Amédro, F., Dupuis, C., González-Donoso, J. M., … Gartner, S. (1993). Sequence stratigraphy in a distal environment: The Cenomanian of the Kalaat Senan region (central Tunisia). *Bulletin des Centres de Recherches Exploration-Production Elf-Aquitaine*, 17(2), 395–433.

Robaszynski, F., Pomerol, B., Masure, E., Bellier, J.-P., & Deconinck, J.-F. (2005). Stratigraphy and stage boundaries in reference sections of the Upper Cretaceous Chalk in the east of the Paris Basin: The "Craie 700" Provins boreholes. *Cretaceous Research*, 26(2), 157–169. https://doi.org/10.1016/j.cretres.2004.10.003

Robaszynski, F., Zagrarni, M. F., Caron, M., & Amédro, F. (2010). The global bio-events at the Cenomanian-Turonian transition in the reduced Bahloul Formation of Bou Ghanem (central Tunisia). *Cretaceous Research*, 31(1), 1–15. https://doi.org/10.1016/j.cretres.2009.07.002

Sahagian, D., Pinous, O., Olferiev, A., & Zakharov, V. (1996). Eustatic curve for the Middle Jurassic–Cretaceous based on Russian Platform and Siberian stratigraphy: Zonal resolution. *AAPG Bulletin*, 80(9), 1433–1458.

Salaj, J. (1996). Tunisian Upper Cretaceous hypostratotypes as possible candidates of Tethyan stratotypes including stratotype boundaries. *Zemni Plyn a Nafta*, 40, 245–307.

Sames, B., Wagreich, M., Conrad, C. P., & Iqbal, S. (2020). Aquifer-eustasy as the main driver of short-term sea-level fluctuations during Cretaceous hothouse climate phases. *Special Publication – Geological Society of London*, 498(1), 9–38. https://doi.org/10.1144/SP498-2019-105

Sames, B., Wagreich, M., Wendler, J. E., Haq, B. U., Conrad, C. P., Melinte-Dobrinescu, M. C., … Zorina, S. O. (2016). Short-term sea-level changes in a greenhouse world–A view from the Cretaceous. *Palaeogeography, Palaeoclimatology, Palaeoecology*, 441, 393–411. https://doi.org/10.1016/j.palaeo.2015.10.045

Schlagintweit, F., & Simmons, M. D. (2022). Developing best practice in micropalaeontology: Examples from the mid-Cretaceous of the Zagros Mountains. *Acta Palaeontologica Romaniae*, 18(2), 63–84. https://doi.org/10.35463/j.apr.2022.02.03

Schmitz, M. D. (2020). Appendix 2: Radioisotope ages used in GTS2020. In F.M. Gradstein, J. G. Ogg, M. D. Schmitz, & G. M. Ogg (Eds.), *Geologic Time Scale 2020* (pp. 1285–1349). Elsevier. https://doi.org/10.1016/B978-0-12-824360-2.00046-2

Scholle, P. A., & Arthur, M. (1980). Carbon isotope fluctuations in Cretaceous pelagic limestones: Potential stratigraphic and petroleum exploration tool. *Bulletin of the American Association of Petroleum Geologists*, 64, 67–87.

Schulze, F. (2003). Growth and crises of the Late Albian – Turonian carbonate platform, west central Jordan: integrated stratigraphy and environmental changes. PhD thesis, Bremen University.

Scopelliti, G., Bellanca, A., Coccioni, R., Luciani, V., Neri, R., Baudin, F., … Marcucci, M. (2004). High-resolution geochemical and biotic records of the Tethyan 'Bonarelli Level' (OAE2, latest Cenomanian) from the Calabianca–Guidaloca composite section, northwestern Sicily, Italy. *Palaeogeography, Palaeoclimatology, Palaeoecology*, 208(3-4), 293–317. https://doi.org/10.1016/j.palaeo.2004.03.012

Scopelliti, G., Bellanca, A., Erba, E., Jenkyns, H. C., Neri, R., Tamagnini, P., … Masetti, D. (2008). Cenomanian–Turonian carbonate and organic-carbon isotope records, biostratigraphy and provenance of a key section in NE Sicily, Italy: Palaeoceanographic and palaeogeographic implications. *Palaeogeography, Palaeoclimatology, Palaeoecology*, 265(1-2), 59–77. https://doi.org/10.1016/j.palaeo.2008.04.022

Scotese, C. R. (2021). An atlas of Phanerozoic paleogeographic maps: The seas come in and the seas go out. *Annual Review of Earth and Planetary Sciences*, 49(1), 679–728. https://doi.org/10.1146/annurev-earth-081320-064052

Scotese, C. R., Song, H., Mills, B. J., & van der Meer, D. G. (2021). Phanerozoic paleotemperatures: The Earth's changing climate during the last 540 million years. *Earth-Science Reviews*, 215, 103503. https://doi.org/10.1016/j.earscirev.2021.103503

Scott, R. W., Oboh-Ikuenobe, F. E., Benson, G. G., Jnr.,, Holbrook, J. M., & Alnahwi, A. (2018). Cenomanian-Turonian flooding cycles: U. S. Gulf Coast and Western

Interior. *Cretaceous Research*, *89*, 191–210. https://doi.org/10.1016/j.cretres.2018.03.027

Scott, R. W., Simo, J. A., & Masse, J. P. (1993). Economic resources in Cretaceous carbonate platforms: an overview. In J. A. Simo, R. W. Scott, & J. P. Masse (Eds.), AAPG Memoir: Vol. *56. Cretaceous Carbonate Platforms* (pp. 15–23). Tulsa, OK. https://doi.org/10.1306/M56578C2

Sigal, J. (1977). Essai de zonation du Crétacé méditerranéen à l'aide des foraminifères planktoniques. *Géologie Méditerranéenne*, *4*(2), 99–107. https://doi.org/10.3406/geolm.1977.997

Simmons, M. D. (2015). Age is an interpretation. In A. Cullum, & A. W. Martinius (eds.), *52 Things You Should Know About Palaeontology* (pp. 26–27). Canada: Agile Libre.

Simmons, M. D. (2021). It's about time. *Newsletter of Micropalaeontology*, *104*, 43–48.

Simmons, M. D., & Bidgood, M. D. (2022). Biostratigraphy: What have we learnt? *Newsletter of Micropalaeontology*, *105*, 57–62.

Simmons, M. D., Miller, K. G., Ray, D. C., Davies, A., van Buchem, F. S. P., & Gréselle, B. (2020). Phanerozoic Eustasy. In F. M. Gradstein, J. G. Ogg, M. D. Schmitz, & G. M. Ogg (Eds.)*, Geologic Time Scale 2020* (pp. 357–400). Elsevier. https://doi.org/10.1016/B978-0-12-824360-2.00013-9

Simmons, M. D., Sharland, P. R., Casey, D. M., Davies, R. B., & Sutcliffe, O. E. (2007). Arabian Plate sequence stratigraphy: Potential implications for global chronostratigraphy. *GeoArabia*, *12*(4), 101–130. https://doi.org/10.2113/geoarabia1204101

Simpson, G. G. (1951). The species concept. *Evolution; International Journal of Organic Evolution*, *5*(4), 285–298. https://doi.org/10.1111/j.1558-5646.1951.tb02788.x

Skelton, P. W. (Ed.). (2003). *The Cretaceous World*. Cambridge University Press.

Sliter, W. V. (1989). Biostratigraphic zonation for Cretaceous planktonic foraminifers examined in thin section. *Journal of Foraminiferal Research*, *19*(1), 1–19. https://doi.org/10.2113/gsjfr.19.1.1

Smirnov, J. P., Moskvin, M. M., & Tkachuk, G. A. (1986). North Caucasus and Pre-Caucasus. In M. M. Aliev, N. A. Krylov, & M. M. Pavlova (Eds.)*, Upper Cretaceous of the south of the USSR* (pp. 22–104). Nauka Moscow.

Sorman, M. G., Fraass, A. J., Huber, B. T., Wiggins, J. W., & Acha, B. (2016). Morphometric study of the *Rotalipora* lineage (planktic foraminifera) during the middle and late Cenomanian. Unpublished poster. Available at:

Spezzaferri, S., & Caron, M. (2008). Revision of the planktonic foraminifera *Pseudothalmanninella klausi* (Lehmann, 1966) and *Globotruncanella semsalensis* (Corminboeuf, 1961) and first scanning electron microscope (SEM) images of the holotypes. *Revue de Paléobiologie*, *27*(1), 81–88.

Sprovieri, M., Sabatino, N., Pelosi, N., Batenburg, S. J., Coccioni, R., Iavarone, M., & Mazzola, S. (2013). Late

Cretaceous orbitally-paced carbon isotope stratigraphy from the Bottaccione Gorge (Italy). *Palaeogeography, Palaeoclimatology, Palaeoecology*, *379–380*, 81–94. https://doi.org/10.1016/j.palaeo.2013.04.006

Stampfli, G. M., & Borel, G. D. (2002). A plate tectonic model for the Paleozoic and Mesozoic constrained by dynamic plate boundaries and restored synthetic oceanic isochrons. *Earth and Planetary Science Letters*, *196* (1–2), 17–33. https://doi.org/10.1016/S0012-821X(01)00588-X

Steuber, T., Scott, R. W., Mitchell, S. F., & Skelton, P. W. (2016). Part N, Revised, Volume 1, Chapter 26C: Stratigraphy and diversity dynamics of Jurassic–Cretaceous Hippuritida (rudist bivalves). *Treatise Online*, *81*, 1–17. https://doi.org/10.17161/to.v0i0.6474

Takashima, R., Nishi, H., Yamanaka, T., Orihashi, Y., Tsujino, Y., Quidelleur, X., … Ando, T. (2019). Establishment of Upper Cretaceous bio- and carbon-isotope stratigraphy in the northwest Pacific Ocean and radiometric ages around the Albian/Cenomanian, Coniacian/Santonian and Santonian/Campanian boundaries. *Newsletters on Stratigraphy*, *52*(3), 341–376. https://doi.org/10.1127/nos/2019/0472

Time Scale Creator (TSC) (2020). Visualization of enhanced Geologic Time Scale 2020 database (Version PRO8.0; 2022) James Ogg (database coordinator)

Torsvik, T. H., & Cocks, L. R. M. (2017). *Earth History and Palaeogeography*. Cambridge University Press. https://doi.org/10.1017/9781316225523

Tremolada, F. (2002). Aptian to Campanian calcareous nannofossil biostratigraphy from the Bottaccione section, Gubbio, Central Italy. *Rivista Italiana di Paleontologia e Stratigrafia*, *108*(3), 441–456.

Troger, K.-A., & Kennedy, W. J. (1996). The Cenomanian stage. *Bulletin de l'Institut Royal des Sciences Naturelles de Belgique*, *66*, 57–68.

Tur, N. A., Smirnov, J. P., & Huber, B. T. (2001). Late Albian–Coniacian planktic foraminifera and biostratigraphy of the northeastern Caucasus. *Cretaceous Research*, *22*(6), 719–734. https://doi.org/10.1006/cres.2001.0295

Van Buchem, F. S. P., Simmons, M. D., Droste, H. J., & Davies, R. B. (2011). Late Aptian to Turonian stratigraphy of the eastern Arabian Plate – depositional sequences and lithostratigraphic nomenclature. *Petroleum Geoscience*, *17*(3), 211–222. https://doi.org/10.1144/1354-079310-061

Van der Meer, D. G., van den Berg van Saparoea, A. V. D. B., Van Hinsbergen, D. J. J., Van de Weg, R. M. B., Godderis, Y., Le Hir, G., & Donnadieu, Y. (2017). Reconstructing first-order changes in sea level during the Phanerozoic and Neoproterozoic using strontium isotopes. *Gondwana Research*, *44*, 22–34. https://doi.org/10.1016/j.gr.2016.11.002

Van Hinte, J. E. (1976). A Cretaceous time scale. *Bulletin of the American Association of Petroleum Geologists*, *60*, 498–516.

Vérard, C., Hochard, C., Baumgartner, P. O., Stampfli, G. M., & Liu, M. (2015). 3D palaeogeographic recon-

structions of the Phanerozoic versus sea-level and Sr-ratio variations. *Journal of Palaeogeography*, *4*(1), 64–84. https://doi.org/10.3724/SP. J.1261.2015.00068

Voigt, S., Gale, A. S., & Flogel, S. (2004). Midlatitude shelf seas in the Cenomanian-Turonian greenhouse world: Temperature evolution and North Atlantic circulation. *Paleoceanography*, *19*(4), 1–17. https://doi.org/10.1029/2004PA001015

Voigt, S., Gale, A. S., & Voigt, T. (2006). Sea-level change, carbon cycling and palaeoclimate during the Late Cenomanian of northwest Europe: An integrated palaeoenvironmental analysis. *Cretaceous Research*, *27*(6), 836–858. https://doi.org/10.1016/j.cretres.2006.04.005

Voigt, S., Gale, A. S., Jung, C., & Jenkyns, H. C. (2012). Global correlation of Upper Campanian-Maastrichtian successions using carbon-isotope stratigraphy: Development of a new Maastrichtian timescale. *Newsletters on Stratigraphy*, *45*(1), 1–25. https://doi.org/10.1127/0078-0421/2012/0016

Wade, B. S., Olsson, R. K., Pearson, P. N., Huber, B. T., & Berggren, W. A. (Eds.)(2018). Atlas of Oligocene Planktonic Foraminifera. *Cushman Foundation for Foraminiferal Research, Special Publication*, *46*.

Wagreich, M., Bojar, A.-V., Sachsenhofer, R. F., Neuhuber, S., & Egger, H. (2008). Calcareous nannoplankton, planktonic foraminiferal, and carbonate carbon isotope stratigraphy of the Cenomanian–Turonian boundary section in the Ultrahelvetic Zone (Eastern Alps, Upper Austria). *Cretaceous Research*, *29*(5-6), 965–975. https://doi.org/10.1016/j.cretres.2008.05.017

Walaszczyk, I., & Cobban, W. A. (2016). Inoceramid bivalves and biostratigraphy of the upper Albian and lower Cenomanian of the United States Western Interior Basin. *Cretaceous Research*, *59*, 30–68. https://doi.org/10.1016/j.cretres.2015.10.019

Wendler, I. (2013). A critical evaluation of carbon isotope stratigraphy and biostratigraphic implications for Late Cretaceous global correlation. *Earth-Science Reviews*, *126*, 116–146. https://doi.org/10.1016/j.earscirev.2013.08.003

Wendler, J. E., & Wendler, I. (2016). What drove sea-level fluctuations during the mid-Cretaceous greenhouse climate? *Palaeogeography, Palaeoclimatology, Palaeoecology*, *441*, 412–419. https://doi.org/10.1016/j.palaeo.2015.08.029

Wendler, J. E., Lehmann, J., & Kuss, J. (2010). Orbital time scale, intra-platform basin correlation, carbon isotope stratigraphy and sea-level history of the Cenomanian Turonian Eastern Levant platform, Jordan. In C. Homberg, & M. Bachman (Eds.), Geological Society, London, Special Publication: Vol. *341*. *Evolution of the Levant Margin and Western Arabia Platform Since the Mesozoic* (pp. 171–186). https://doi.org/10.1144/SP341.8

Wendler, J. E., Meyers, S. R., Wendler, I., & Kuss, J. (2014). A million year-scale astronomical control on Late Cretaceous sea-level. *Newsletters on Stratigraphy*, *47*(1), 1–19. https://doi.org/10.1127/0078-0421/2014/0038

Wilmsen, M. (2007). Integrated stratigraphy of the upper Lower – lower Middle Cenomanian of northern Germany and southern England. *Acta Geologica Polonica*, *57*(3), 263–279.

Wonders, A. A. H. (1978). Phylogeny, classification and biostratigraphic distribution of keeled Rotaliporinae. *Proceedings of the Koninklijke Nederlandse Akademie van Wetenschappen. Series B, Palaeontology, Geology, Physics and Chemistry*, *81*, 113–144.

Wonders, A. A. H. (1980). Middle and Late Cretaceous planktonic foraminifera of the Western Mediterranean area. *Utrecht Micropaleontology Bulletin*, *24*, 1–158.

Wright, C. W., Kennedy, W. J., & Gale, A. S. (2017). The Ammonoidea of the Lower Chalk. Part 7. *Palaeontographical Society*, *171*, 461–571.

Wright, N. M., Seton, M., Williams, S. E., Whittaker, J. M., & Müller, R. D. (2020). Sea level fluctuations driven by changes in global ocean basin volume following supercontinent break-up. *Earth-Science Reviews*, *208*, 103293. https://doi.org/10.1016/j.earscirev.2020.103293

Appendix 1

Some uppermost Albian, Cenomanian, and lower Turonian Rotaliporids* and other stratigraphically useful taxa (genus assignment as per 'Mikrotax'; Huber et al. 2016). * For a treatment on the separation of the genera *Rotalipora*, *Thalmanninella*, *Pseudothalmanninella*, *Anaticinella* and *Pseudorotalipora* see Gonzalez-Donoso et al. (2007).

Taxon or marker	Taxonomic Status Recommended Reference(s)	Most Likely Maximum Stratigraphic Range (with ammonite or foraminifera zones where possible)	Comments on calibration and biostratigraphic utility
Helvetoglobotruncana helvetica (Bolli, 1945)	Huber and Petrizzo (2014)	Lower Turonian (*devonense* zone) to middle Turonian (*woolgari* zone). [Marker for the *H. helvetica* TRZ]. Local FADs can occur at Peak 'C' of OAE2 and considerably higher (Falzoni et al. 2018).	FAD appears very diachronous and "highly unreliable" because of taxonomy/ species concept issues and transitional forms with *H. praehelvetica* (ancestor species). (Huber and Petrizzo 2014, Falzoni et al. 2018, Gale et al. 2018).
Helvetoglobotruncana praehelvetica (Trujillo, 1960)	Huber and Petrizzo (2014)	Upper Cenomanian (*guerangeri/geslinianum* zones?) to middle Turonian (*woolgari* zone). Local FADs can occur above, at, or below Peak 'A' of OAE2 (Falzoni et al. 2018).	FAD diachronous and "unreliable" because of taxonomy/species concept issues and transitional forms with *W. aprica* (ancestor species). (Huber and Petrizzo 2014, Falzoni et al. 2018)
Onset of 'Heterohelicid shift'	See Falzoni et al. (2018) for a description and review.	Upper Cenomanian (*geslinianum* zone = uppermost *R. cushmani* zone. Lowest FAD recorded co-incident with Peak 'A' of OAE2 (Bomou in Falzoni et al. 2018).	A regional/global upwards increase in heterohelicids to >50 % of the planktonic foraminifera assemblage thought to be relatively synchronous although exact placement may rely on measurements based on either 3D or thin-section observations (see Falzoni et al. 2018).
'P/B Break'	Jarvis et al. (2006), Joo and Sageman (2014)	Middle Cenomanian (mid-*rhotomagense* zone)	A biostratigraphic event involving an abrupt upwards increase in the proportion of planktonic forams in assemblages widely recorded globally. There is sometimes also a small $\delta^{13}C$ event associated with the change, calibrated to the mid *rhotomagense* ammonite zone (e. g., Jarvis et al. 2006).
Rotalipora cushmani (Morrow, 1934)	Caron and Spezzaferri (2006), Gilardoni (2017)	Upper middle Cenomanian (*rhotomagense* zone) (Petrizzo and Gilardoni 2020) to uppermost Cenomanian (*geslinianum* zone) [marker for the *R. cushmani* TRZ]. LAD commonly lies between Peaks 'A' and 'B' of OAE2 (Falzoni et al. 2018).	The FAD of *R. cushmani* is controversial, placed by some (e. g., Premoli Silva and Sliter 1995, Coccioni and Galeotti 2003, Coccioni and Premoli Silva 2015) well down in the lower Cenomanian. These records are probably not true *R. cushmani* s. s. (see text). The FAD is more likely to occur within the middle Cenomanian (Eldrett et al. 2015, Petrizzo and Gilardoni 2020) specifically the *rhotomagense* (middle Cenomanian) ammonite zone (Jarvis et al. 2006). Atypical forms of *R. cushmani* are widely recorded above the nominal FAD (e. g.,

Taxon or marker	Taxonomic Status Recommended Reference(s)	Most Likely Maximum Stratigraphic Range (with ammonite or foraminifera zones where possible)	Comments on calibration and biostratigraphic utility
			Desmares et al. 2007) and attributed to the "*degradation of the species at global scale in response to the expansion of the oxygen minimum zone*" (i. e., the onset of OAE2). Although the LAD is regarded as reliable, it is likely to be somewhat diachronous in the WIB (Falzoni et al. 2018)
Rotalipora montsalvensis (Mornod, 1950)	Caron (1976), Caron and Spezzaferri (2006), Gilardoni (2017)	Lower Cenomanian (*mantelli-dixoni* zones) (Caron and Spezzaferri 2006, Gonzalez-Donoso et al. 2007) to upper Cenomanian (?*guerangeri-geslinianum* zones) (Falzoni et al. 2018).	LAD is usually below that of *R. cushmani*. Regarded as the ancestor of *R. cushmani* but considered as within the variability of *R. cushmani* by Georgescu (2017) which effectively (and unrealistically) lowers the FAD of that species to the lower Cenomanian, but as a separate (and ancestral) species by Gonzalez-Donoso et al. (2007) and Petrizzo and Gilardoni (2020). The latter authors regard the FAD of *R. montsalvensis* as "unreliable" as they found the FAD to occur closer to the *T. reicheli* zone in their material.
Rotalipora praemontsalvensis Ion, 1976	Gonzalez-Donoso et al. (2007), Sorman et al. (2016), Huber et al. 2016 ('Mikrotax')	Lower middle Cenomanian *inerme* zone) (Gonzalez-Donoso et al. 2007, Huber et al. 2016 'Mikrotax') to upper Cenomanian (?*guerangeri-geslinianum* zones) (Falzoni et al. 2018)	The stratigraphic range of this seldom recorded species with respect to *R. montsalvensis* (i. e., either as ancestor or descendant) is debated (see Gonzalez-Donoso et al. 2007).
Thalmanninella appenninica (Renz, 1936)	Petrizzo and Huber (2006), Ando and Huber (2007), Gonzalez-Donoso et al. (2007), Petrizzo and Gilardoni (2020)	Upper Albian (upper *fallax* zone) [marker for base *T. appenninica* zone] to upper Cenomanian (approx. *guerangeri* zone) (Petrizzo and Gilardoni 2020).	Gonzalez-Donoso et al. (2007) recognise three typological forms, *T. appenninica*, *T. appenninica* cylindrical and *T. appenninica* umbilico-convex, which they say belong to two different lineages.
Thalmanninella balernaensis (Gandolfi, 1957)	Petrizzo and Huber (2006), Gonzalez-Donoso et al. (2007)	Upper Albian to lower Cenomanian (probably *dixoni* zone) (Petrizzo and Gilardoni 2020).	Gonzalez-Donoso et al. (2007) recognise two typological forms, *T. balernaensis* and *T. balernaensis* umbilico-convex, which they say belong to different lineages. See also Petrizzo et al. (2015). LAD placed in the *T. globotruncanoides* zone by Petrizzo and Gilardoni (2020). Considered as a junior synonym of *T. appenninica* for a period of time.
Thalmanninella brotzeni Sigal, 1948	Petrizzo et al. (2015)	Upper Albian (*briacensis* zone) (Petrizzo et al. 2015) to lower upper Cenomanian (prob. *guerangeri* zone) (Falzoni et al. 2018).	Synonymised with *T. globotruncanoides* for a significant time. Admittedly the morphologies of the two species are very similar (see Petrizzo et al. 2015, Fig 3).

Taxon or marker	Taxonomic Status Recommended Reference(s)	Most Likely Maximum Stratigraphic Range (with ammonite or foraminifera zones where possible)	Comments on calibration and biostratigraphic utility
Thalmanninella deeckei (Franke, 1925)	Ando and Huber (2007)	Upper Cenomanian (mid-upper *R. cushmani* zone (Petrizzo and Gilardoni 2020). The LAD occurs at various points along the inflection leading up to Peak 'A' (OAE2) on the δ^{13}C curve (low – e. g., Bomou et al. 2013, Falzoni et al. 2016) or higher e. g., Falzoni et al. 2018).	LAD always occurs just below the LAD of *Th. greenhornensis* and is regarded as reliable (Falzoni et al. 2018). The FAD is always above the LAD of *T. reicheli* but morphological similarities can make distinguishing the two species difficult, especially in thin section.
Thalmanninella evoluta Sigal, 1969	Petrizzo and Huber (2006), Petrizzo and Gilardoni (2020)	Upper Albian to lower/? middle Cenomanian	A seldom used taxon often placed in synonymy with other species.
Thalmanninella gandolfii (Luterbacher and Premoli Silva, 1962)	Gonzalez-Donoso et al. (2007)	Uppermost Albian (*briacensis* zone, close to the FAD of *T. brotzeni*) to upper Cenomanian (see Petrizzo and Gilardoni 2020 who regard these events as unreliable)	Not previously thought to range above the lower Cenomanian but recorded from the *R. cushmani* zone by Petrizzo and Gilardoni (2020).
Thalmanninella globotruncanoides (Sigal, 1948)	Petrizzo et al. (2015)	Base Cenomanian GSSP marker (intra-*briacensis* zone) [marker for base *T. globotruncanoides* zone] (Kennedy et al. 2004, Gale et al. 2020) to middle Cenomanian (Petrizzo and Gilardoni 2020)	Included junior synonym *T. brotzeni* for a significant time (see above) but now considered separate. It is usually rare in the lowest part of its range becoming common shortly after its inception.
Thalmanninella greenhornensis (Morrow, 1934)	Ando and Huber (2007), Petrizzo and Gilardoni (2020)	Upper lower Cenomanian (intra-*dixoni* zone) to upper Cenomanian (*geslinianum* zone) (Petrizzo and Gilardoni 2020). The LAD occurs at or just below Peak 'A' of OAE2.	FAD coincident or very close to that of *T. reicheli* (where both species are found together) although *T. greenhornensis* is more common and widespread. The *T. greenhornensis* zone is associated with the δ^{13}C isotope peaks of the MCE (Petrizzo and Gilardoni 2020). The FAD event is difficult to calibrate precisely to the timescale but occurs approximately 10 m below the MCE event at Monte Petrano. Since the MCE begins in the *inerme* ammonite zone it is likely that the FAD lies within the upper *dixoni* ammonite zone. The LAD almost always occurs just below that of *R. cushmani* and is considered reliable by Falzoni et al. (2018).

Taxon or marker	Taxonomic Status Recommended Reference(s)	Most Likely Maximum Stratigraphic Range (with ammonite or foraminifera zones where possible)	Comments on calibration and biostratigraphic utility
Thalmanninella micheli (Sacal and Debourle, 1957)	See Gonzalez-Donoso et al. (2007), Premoli Silva and Verga (2004) and Premoli Silva and Sliter (1995)	Lower Cenomanian (lower *mantelli* zone) (Gonzalez-Donoso et al. 2007, Lipson-Benitah 2008) to upper Cenomanian (*guerangeri-geslinianum* zones) (Caron and Spezzaferri 2006)	A sporadically occurring (or under-reported) species often confused with *T. reicheli*.
Thalmanninella praebalernaensis (Sigal, 1969)	Petrizzo and Huber (2006)	Upper Albian	Not usually recorded above the Albian in the literature (e. g., Gonzalez-Donoso et al. 2007, Lipson-Benitah 2008, Gale et al. 2011) The LAD reported from "*within the T. globotruncanoides zone*" by Huber et al. (2016 – 'Mikrotax') is considered incorrect as a result of a mistake during web-page compilation.
Thalmanninella reicheli (Mornod, 1950)	Caron (1976), Caron and Spezzaferri (2006)	Lower Cenomanian (upper part, near top *dixoni* zone) to upper Cenomanian (lower part) (*guerangeri* zone) (Petrizzo and Gilardoni 2020)	Rarity, problems with identification and restricted geographical distribution renders *T. reicheli* unsuitable for correlation outside the Mediterranean area. The (former) *T. reicheli* zone is associated with the two $\delta^{13}C$ isotope peaks of MCE (I) (Ando et al. 2009, Petrizzo and Gilardoni 2020). FAD (where found) is often very close to the FAD of *T. greenhornensis* (see above).
Pseudothalmanninella klausi (Lehmann, 1966)	Spezzaferri and Caron (2008)	LAD is uppermost Albian (*T. appenninica* zone) (Spezzaferri and Caron 2008).	Not commonly reported but could be a useful marker for the *T. appenninica* zone at the top of the Albian.
Pseudothalmanninella tehamaensis (Marianos and Zingula, 1966)	Petrizzo et al. (2015). See also Petrizzo and Gilardoni (2020)	Intra-upper Albian to lower middle Cenomanian (Petrizzo et al. 2015, Petrizzo and Gilardoni 2020).	The taxonomic status of this species has been 'fluid' (see Petrizzo et al. 2015). Its FAD was once cited as a secondary marker for the base Cenomanian (Kennedy et al. 2004) but is diachronous, occurring much lower (Petrizzo et al. 2015). It was also thought not to range above the lowermost Cenomanian (Petrizzo et al. 2015). However, a few specimens have been recorded from the *T. greenhornensis* zone of Petrizzo and Gilardoni (2020) [formerly *broadly* equivalent to the *T. reicheli* zone]. However, the same authors state the species is unreliable for correlation.
Pseudothalmanninella ticinensis (Gandolfi, 1942)	See Ando and Huber (2007), Gonzalez-Donoso et al. (2007)	Intra-upper Albian to earliest Cenomanian (*briacensis*–? *mantelli* zones) (Petrizzo and Gilardoni 2020).	Thought not to exist above the top Albian for a long time but found overlapping with *T. globotruncanoides* in DSDP hole 547A and Monte Petrano, Italy (Petrizzo and Gilardoni 2020). However, Petrizzo and Gilardoni consider the LAD of *P. ticinensis* to be an "*unreliable bioevent*".

Taxon or marker	Taxonomic Status Recommended Reference(s)	Most Likely Maximum Stratigraphic Range (with ammonite or foraminifera zones where possible)	Comments on calibration and biostratigraphic utility
Ticinella madecassiana Sigal, 1966	See Huber et al. (2016 – 'Mikrotax'), Petrizzo and Gilardoni (2020)	Intra-lower Albian to lowermost Cenomanian (*briacensis-?mantelli* zones) (Petrizzo and Gilardoni 2020).	Thought not to exist above the top Albian for a long time but found overlapping with *T. globotruncanoides* in DSDP hole 547A, Monte Petrano and Le Brecce, Italy (Petrizzo and Gilardoni 2020) and by Gale et al. (2021) in Morocco. However, Petrizzo and Gilardoni consider the LAD of *T. madecassiana* to be an "*unreliable bioevent*".
Ticinella primula Luterbacher in Renz et al., 1963	See Huber et al. (2016) ('Mikrotax') and Huber et al. (2022)	Intra-lower Albian to lowermost Cenomanian (*briacensis-?mantelli* zones) (Petrizzo and Gilardoni 2020).	Thought not to exist above the top Albian for a long time (and see Huber et al. 2022) but found overlapping with *T. globotruncanoides* in DSDP hole 547A, Monte Petrano and Le Brecce, Italy (Petrizzo and Gilardoni 2020). However, the same authors consider the LAD of *T. primula* to be an "*unreliable bioevent*".
Biticinella breggiensis (Gandolfi, 1942)	Gale et al. (2011)	Middle Albian to upper Albian (near top *T. appenninica* zone) (Gilardoni 2017, Huber et al. 2022).	LAD occurs close to the top of the Albian stage (*T. appenninica* zone) but usually below the LAD of *P. buxtorfi* (Gilardoni 2017).
Anaticinella multiloculata (Morrow, 1934)	See Desmares et al. (2007), Falzoni et al. (2018)	Upper Cenomanian (*guerangeri-juddi* zone), Max LAD very close to Cenomanian-Turonian boundary (Caron et al. 2006) although Falzoni et al. (2018) regards the event as diachronous).	Directly descended from *T. greenhornensis* (Ando and Huber 2007, Gonzalez-Donoso et al. 2007) and synonymised under that genus. The taxonomic position of this species requires a full review. Common in, but not necessarily restricted to, the WIB.
Anaticinella planoconvexa (Longoria, 1973)	See Desmares et al. (2007), Falzoni et al. (2018)	Upper Cenomanian (*guerangeri-juddi* zone), Max LAD very close to Cenomanian-Turonian boundary (Caron et al. 2006) although Falzoni et al. (2018) regards the event as diachronous).	Descended from *R. cushmani* (Caron et al. 2006, Desmares et al. 2008) and synonymised under that genus (Gonzalez-Donoso et al. 2007). The taxonomic position of this species requires a full review. Common in, but not necessarily restricted to, the WIB.
Marginotruncana schneegansi (Sigal, 1952)	Robaszynski and Caron (1979), see also Huber et al. (2016 – 'Mikrotax')	Near base Turonian to Santonian (Falzoni et al. 2018).	Regarded as a potentially useful marker by Falzoni et al. (2018), its FAD seems to occur very close to the chronostratigraphic base Turonian and around the $\delta^{13}C$ peak of OAE2 in low latitudes.
Marginotruncana sigali (Reichel, 1950)	Robaszynski and Caron (1979), see also Huber et al. (2016 – 'Mikrotax')	Lower Turonian to Santonian (Falzoni et al. 2018).	Regarded as a potentially useful marker by Falzoni et al. (2018), but only perhaps in low latitudes (FAD is highest at Pueblo) its lowest FAD seems to occur just above the chronostratigraphic base Turonian between Peak 'C' of OAE2 and the 'Holywell' peak.

Taxon or marker	Taxonomic Status Recommended Reference(s)	Most Likely Maximum Stratigraphic Range (with ammonite or foraminifera zones where possible)	Comments on calibration and biostratigraphic utility
Dicarinella hagni (Scheibnerova, 1962)	Robaszynski and Caron (1979), see also Huber et al. (2016 – 'Mikrotax')	Upper Cenomanian (intra-*R. cushmani* zone) to Coniacian (Falzoni et al. 2018).	Regarded as a reliable marker by Falzoni et al. (2018) its FAD occurs below the LADs of *T. greenhornensis* and *T. deeckei* and is often close to the FAD of *D. imbricata* (see also Caron et al. 2006). These events occur below the point where δ^{13}C isotope curve deflects to the right to begin to form peak A of OAE2.
Dicarinella imbricata (Mornod, 1950)	Robaszynski and Caron (1979), see also Huber et al. (2016 – 'Mikrotax')	Upper Cenomanian (intra-*R. cushmani* zone) to Coniacian (Falzoni et al. 2018).	Regarded as a reliable marker by Falzoni et al. (2018) its FAD occurs below the LADs of *T. greenhornensis* and *T. deeckei* and is often close to the FAD of *D. hagni* (see also Caron et al. 2006). These events occur below the point where δ^{13}C isotope curve deflects to the right to begin to form peak A of OAE2.
Praeglobotruncana algeriana (Caron, 1966)	Falzoni et al. (2016)	Upper Cenomanian (intra-*R. cushmani* zone) to upper Turonian (Falzoni et al. 2018).	Regarded as a potentially useful marker by Falzoni et al. (2016, 2018), its FAD seems to occur just below those of *D. imbricata* and *D. hagni* (see also Caron et al. 2006). It can easily be confused with *P. pseudoalgeriana* (Falzoni et al. 2016).
Planomalina buxtorfi (Gandolfi, 1942)	see Huber et al. (2016 – 'Mikrotax') and Gilardoni (2017)	Upper Albian (base of *T. appenninica* zone to near top of the same zone) (Gilardoni 2017, Huber et al. 2022).	LAD occurs close to the top of the Albian stage (*T. appenninica* zone) (Gilardoni 2017).
Laeviella bentonensis (Morrow, 1934)	see Huber et al. (2016 – 'Mikrotax' and Huber et al. 2022)	Middle Albian to uppermost Cenomanian (lowermost *W. archaeocretacea* zone). Max LAD occurs just above Peak 'B' in OAE2 (Falzoni et al. 2018).	A reliable biovent (Falzoni et al. 2018). The highest LAD is just above that of *R. cushmani* (Gale et al. 2018). The FAD of its descendant species *L. bolli* (Pessagno) may lie close to this event (Huber et al. 2022).